NAVAL FACILITIES ENGINEERING SERVICE CENTER
Port Hueneme, California 93043-4370

Technical Report
TR-2097-ENV

FEASIBILITY OF CLEANING PCB CONTAMINATED SURFACES USING PULSED CORONA DISCHARGES

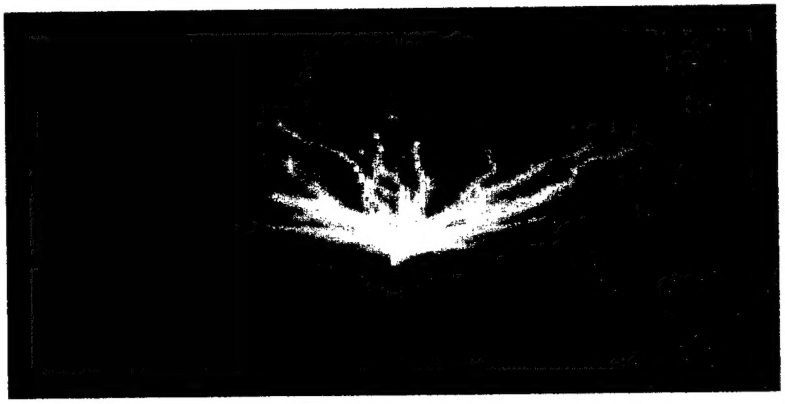

by

Richard E. Kirts

Sponsored by
Office of Naval Research

March 1999

REPORT DOCUMENTATION PAGE

Form Approved
OMB No. 0704-018

1. AGENCY USE ONLY *(Leave blank)*	2. REPORT DATE	3. REPORT TYPE AND DATES COVERED
	March 1999	Final; FY97 - FY98

4. TITLE AND SUBTITLE
FEASIBILITY OF CLEANING PCB CONTAMINATED SURFACES USING PULSED CORONA DISCHARGES

5. FUNDING NUMBERS

6. AUTHOR(S)

Richard E. Kirts

7. PERFORMING ORGANIZATION NAME(S) AND ADDRESSE(S)

Naval Facilities Engineering Service Center
1100 23rd Ave.
Port Hueneme, CA 93043-4370

8. PERFORMING ORGANIZATION REPORT NUMBER

TR-2097-ENV

9. SPONSORING/MONITORING AGENCY NAME(S) AND ADDRESSES

Office of Naval Research
Alexandria, VA

10. SPONSORING/MONITORING AGENCY REPORT NUMBER

11. SUPPLEMENTARY NOTES

12a. DISTRIBUTION/AVAILABILITY STATEMENT

Approved for public release; distribution is unlimited.

12b. DISTRIBUTION CODE

13. ABSTRACT *(Maximum 200 words)*

The objective of this study was to investigate the feasibility of using pulsed corona discharges to destroy organic contaminants on surfaces. Pulsed corona discharge technology uses brief pulses of high voltage to generate strong oxidizing chemicals such as hydroxyl radical and ozone. These chemical species, in aqueous solution, can mineralize organic contaminants in solution or on the surface of solids. The target organic contaminants for this study were polychlorinated biphenyls (PCB) found on parts removed from Navy ships being recycled. Initial studies were performed using phenol as a surrogate for PCBs. Following successful degradation of phenol, degradation of a chlorinated phenol, and finally a chlorinated biphenyl would be studied. The author found no conclusive evidence that pulsed streaming corona discharges significantly degrade phenol. The reason for this is that the experimental procedure did not generate significant amounts of either ozone or hydrogen peroxide. Other investigators have found that up to 25 percent of phenol can be converted into catechol and resorcinol by the pulsed streaming corona discharge process. Catechol and resorcinol are classified as hazardous substances. It was recommended that the project be terminated.

14. SUBJECT TERMS	15. NUMBER OF PAGES
PCB contaminated surfaces, pulsed corona discharges, organic contaminants	
	16. PRICE CODE

17. SECURITY CLASSIFICATION OF REPORT	18. SECURITY CLASSIFICATION OF THIS PAGE	19. SECURITY CLASSIFICATION OF ABSTRACT	
Unclassified	Unclassified	Unclassified	UL

CONTENTS

SUMMARY AND CONCLUSIONS

A test apparatus was designed and built to evaluate the feasibility of using pulsed streaming corona discharges to degrade or mineralize PCBs. Fifty-eight experiments were performed using aqueous solutions of organic dyes as surrogate wastes. The purpose of these experiments was to determine the optimum system configuration. The optimized system configuration was then used to investigate the degradation of phenol by pulsed streaming corona discharges. Phenol was selected a waste surrogate because phenol has the basic benzene ring structure of a chlorinated. Ninety experiments were performed using phenol solutions as surrogate wastes. Little or no degradation of phenol was observed. The degradation of chlorinated phenols and chlorinated biphenyls was not evaluated.

Because the rapid and efficient conversion of phenol into harmless compounds could not be demonstrated, it was recommended to the program manager that this investigation be terminated.

OBJECTIVE

The objective of this study was to investigate a chemical method of destroying organic contamination on surfaces. Of special interest are surfaces of painted metal parts removed from recycled Navy ships. These surfaces are often contaminated with polychlorinated biphenyls (PCB) that render the part a hazardous waste item. The proposed method would destroy contaminants by oxidizing them at the surface rather than removing the surface layer by mechanical or thermal methods.

It has been postulated that pulsed streaming corona discharges generate strong oxidizing chemicals (such as hydroxyl radicals, ozone, and hydrogen peroxide) by means of a specific type of electrical discharge in water. Assuming this postulation is correct, a part cleaning system is envisioned in which the part is immersed in a water bath containing high concentrations of these strong oxidizers. It may be advantageous to add an inexpensive co-reactant (ferrous iron) to the solution to convert hydrogen peroxide to hydroxyl radical. The method offers potential advantages of operation at ambient temperature and pressure, simplicity of design, and use of inexpensive materials of construction.

If the proposed method of treating PCB contaminated ship parts is effective, the cost of manual removal of contaminated materials from ships could be substantially reduced. Handling and disposal costs for the contaminated materials would also be substantially reduced because there would be less hazardous material to collect, manifest, transport, and treat. In addition, metals and other materials that are now being disposed in hazardous waste landfills could be sold to recycling firms.

Current PCB disposal costs average $525,000 for an SSBN and $305,000 for an SSN. If the proposed process can be developed in time to treat 50 submarines (of the remaining 66 scheduled to be recycled) and if the savings in removal and disposal cost per boat is $300,000, then a life-cycle savings of $15 M could be realized.

BACKGROUND

The Navy is currently decommissioning ships at a rate unequaled since the close of World War II. Many of these ships contain polychlorinated biphenyl (PCB) in materials such as paint, acoustic damping felt, oils, gaskets, and electrical cable insulation. PCBs are toxic, and the handling, treatment, and disposal of these wastes is closely regulated by the Toxic Substances Control Act (TSCA) (40 CFR Part 761, Federal Citation 15, USC §2601, and et seq.). The Navy has requested legislation that would largely exempt the armed services from regulations that address cleanup and disposal of *non-liquid* PCBs. However, a recent letter from the Head, Toxic Substances Division, U.S. Environmental Protection Agency, (Ref. 1) recommends proposed amendments to TSCA legislation be passed without the changes requested by the Navy. This means the Navy will continue to be required to clean decommissioned ships of PCBs to the low levels set by current law. At the present time this is an expensive, time consuming, process.

The problem of removal and treatment of PCB contaminated wastes is especially acute at Puget Sound Naval Shipyard (PSNSY) where the Navy is scrapping numerous decommissioned submarines (Figures 1 and 2).

Current cleaning methods remove PCB contaminated paint from a surface with abrasive blasting. Small parts are sometimes cleaned by hand (Figure 3).

The contaminated paint chips, acoustic damping felts, and other PCB wastes are packaged and manifested for disposal by contract. Most of these wastes are buried in a TSCA landfill. Cleaned scrap is sold to recycling firms. In calendar year 1995, PCB contaminated debris from hull cleaning totaled 8.3 million pounds and disposal cost was $5 million.

A cleaning process that mineralizes PCBs at the surface of the part would reduce the expense of contaminant removal, waste handling, and waste disposal, and result in significant cost savings.

The part to be cleaned would be placed in a tank. Oxidizing fluid, generated in a separate apparatus, would be flowed over the piece, and mineralize the PCBs on the surface of the part. Repeated treatment may be required to mineralize PCBs that subsequently migrate to the surface through the paint layer or pores in the metal. The proposed treatment process is based on the assumption that if PCBs are mobile enough to be removed by a solvent soaked swipe for the EPA "patch" test for PCB contamination, the PCBs are susceptible to oxidation by water borne chemicals.

There are other potential applications for a surface cleaning process, such as cleaning organic matter from ship's heat exchanger tubes, cleaning electronic equipment, and cleaning optical components. The process could also mineralize organic compounds in aqueous solution, for example organic compounds in industrial waste waters.

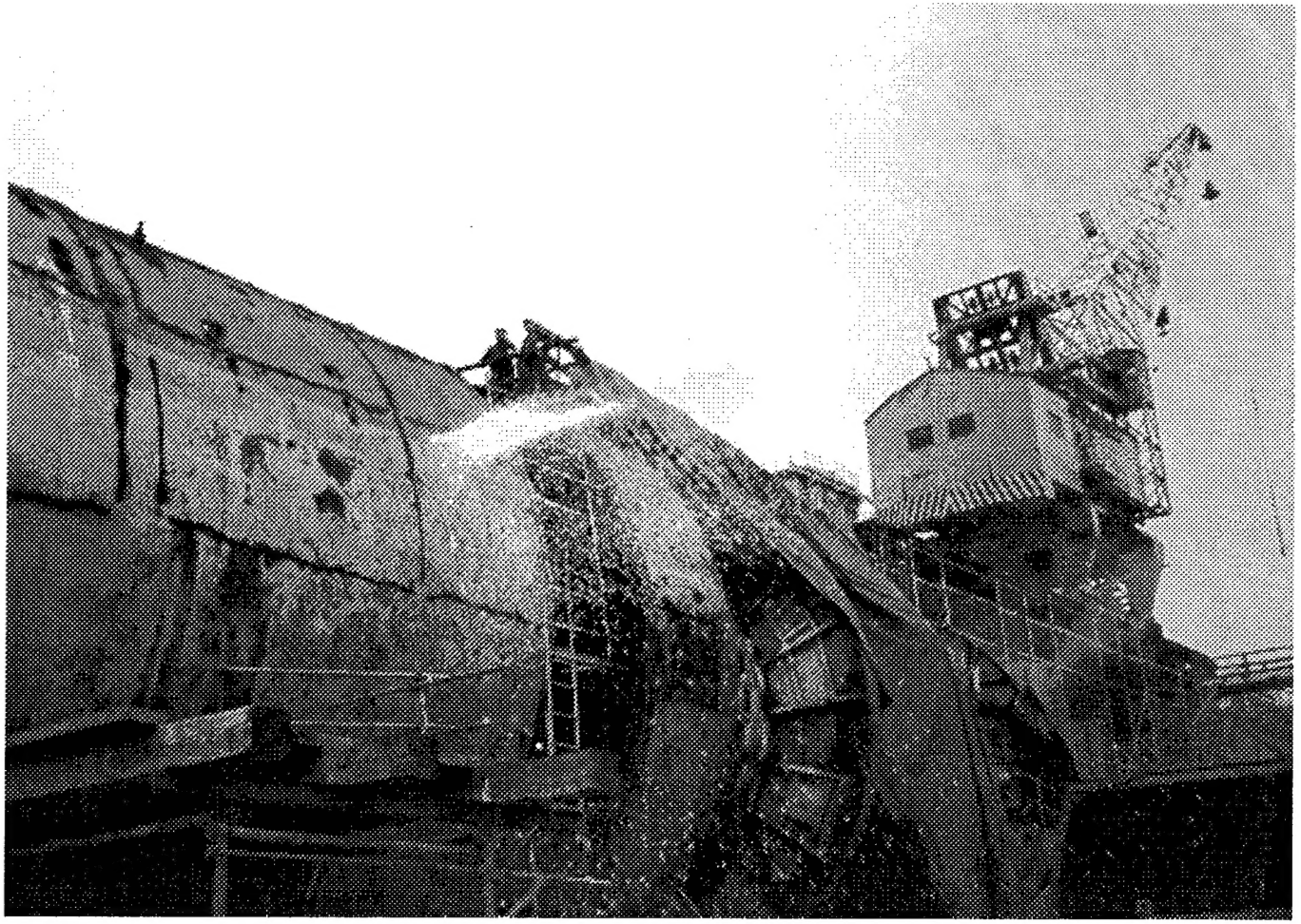

Figure 1. Submarine Being Cut Up for Disposal

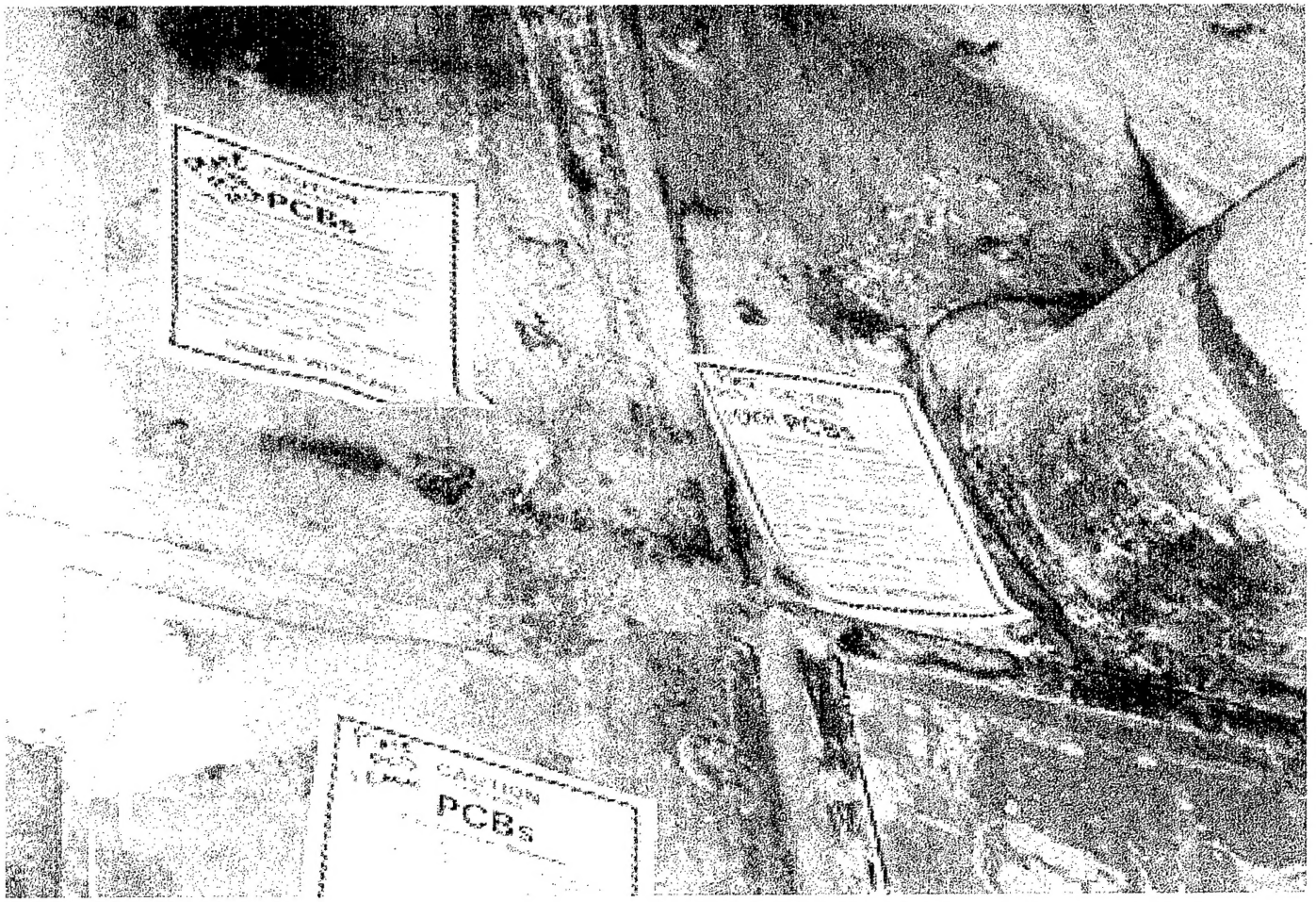

Figure 2. PCB Warning Labels on Painted Surfaces of Submarine Interior

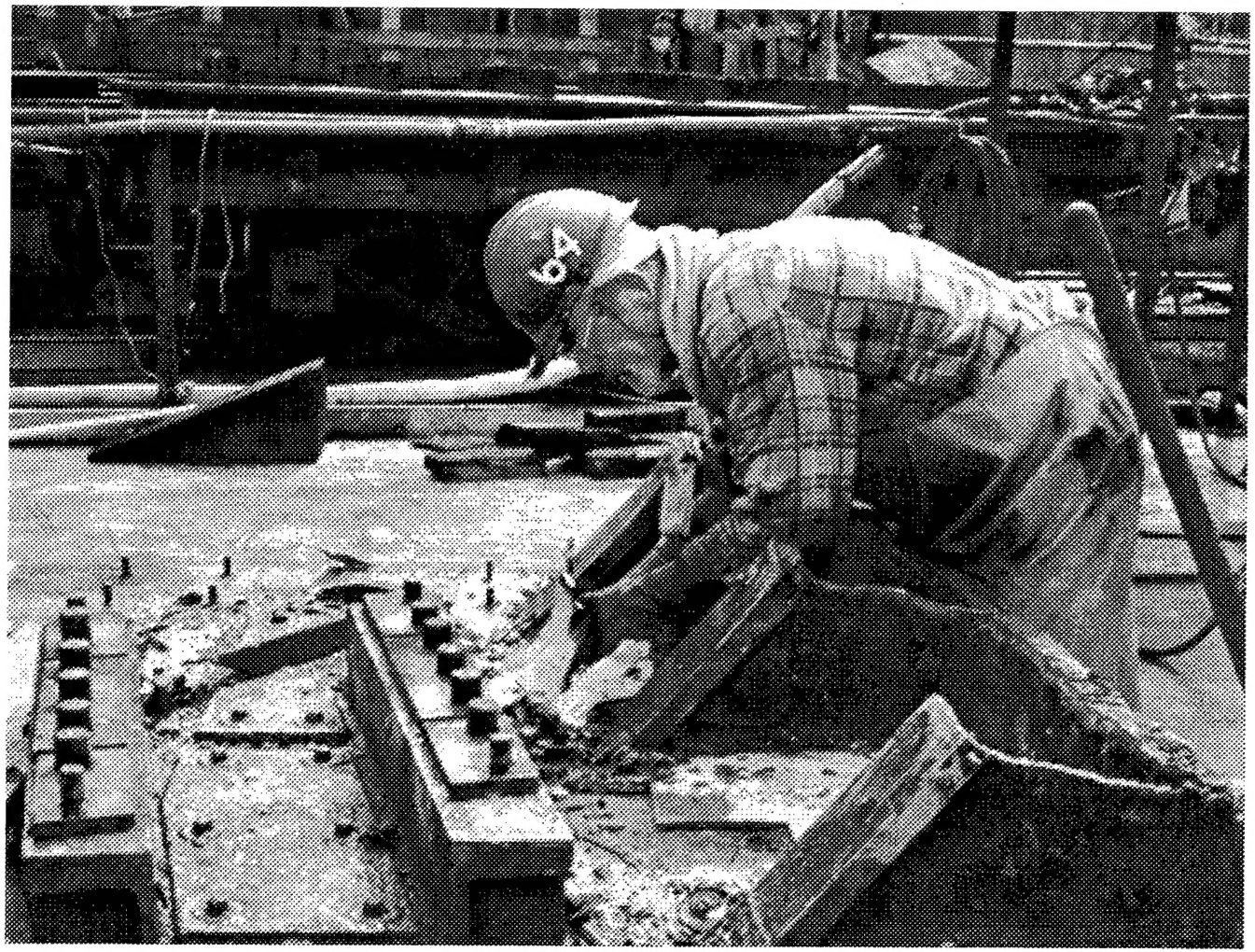

Figure 3. Cleaning Painted Surfaces by Hand

The Office of Naval Research, through the Environmental Applied Research Program, funded this effort.

This work supports the Tri-service Environmental Quality R&D Strategic Plan under requirement 2.III.1.g, "Treatment of PCB Contaminated Equipment." It also supports the CNO's (N091) S&T requirements under requirements 12.1.1, "Develop improved processes for waste minimization, in ordnance manufacturing and demilitarization," and 12.2.a, "Develop non hazardous, and environmentally compliant, safe substitutes for hazardous materials and processes, including hazardous discharge in hull cleaning."

APPROACH

The electrochemical method to be investigated is pulsed corona discharges in water.

The fundamental corona discharge treatment process is illustrated in Figure 4.

The small radius of curvature at the corona discharge point produces the high intensity electric field required to accelerate electrons to a sufficient velocity to convert neutral molecules, such as oxygen and water, into oxidizing species such as ozone and hydroxyl radicals.

The selected corona discharge technology employs very short electrical pulses (typically 50-1500 nanoseconds) to accelerate electrons in the vicinity of the discharge point. These short pulses produce a corona that differs substantially from those produced by long-pulse discharge coronas. Because the mass of an electron is much smaller than the mass of an ion, the very brief pulse of electrical energy maximizes the proportion of the input energy used to accelerate free electrons and minimizes the energy wasted on accelerating ionized species. Ions do not contribute to radical formation, but energetic electrons do.

The high-energy electrons undergo inelastic collisions with the neutral particles of the process medium, which results in a change in the impacted molecule such as electron addition, ionization, dissociation, or excitation. If oxygen or water is present in the process stream, powerful oxidizing compounds such as ozone, atomic oxygen, and the hydroxyl radical are produced. These chemicals are the actual agents that oxidize organic materials. Some of these reaction products are very short lived, but ozone and hydrogen peroxide have been shown to have lives of tens of seconds.

One method of using corona discharge technology to destroy organic compounds in aqueous solution was studied at Florida State University (Ref. 2). A sketch of the Florida State apparatus is shown in Figure 5. The streamer discharge geometry is that of a sharply pointed electrode perpendicular to a grounded disk. In this system, gases can be injected into the solution through the tip of the needle.

Some experimental results from the FSU pulsed corona discharge system are presented Figure 6 (Ref. 2). The data show the breakdown of phenol. Details of the products of decomposition of phenol are not presented in Ref. 2.

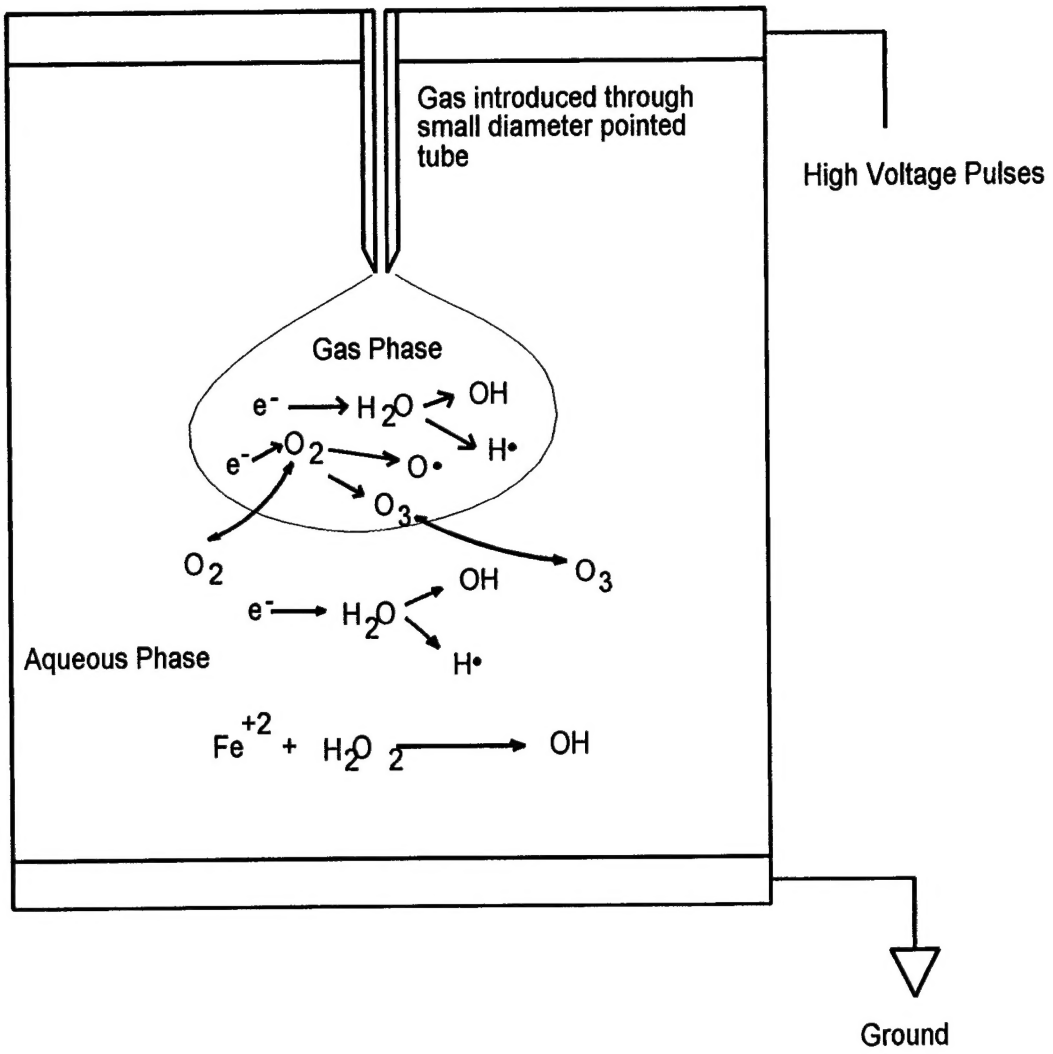

Figure 4 Proposed Mechanism of Corona Discharge Reactions

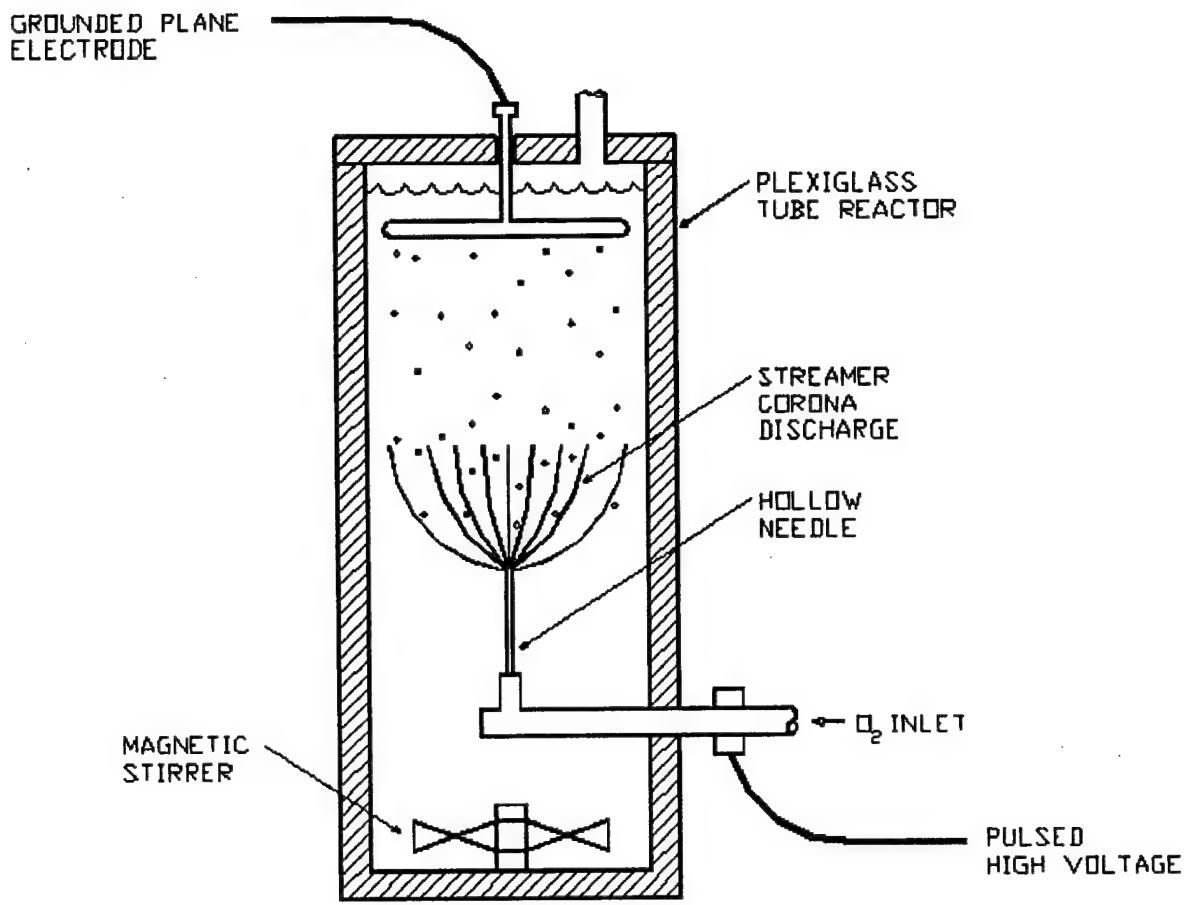

Figure 5. Sketch of Plasma Discharge Apparatus used by Florida State University

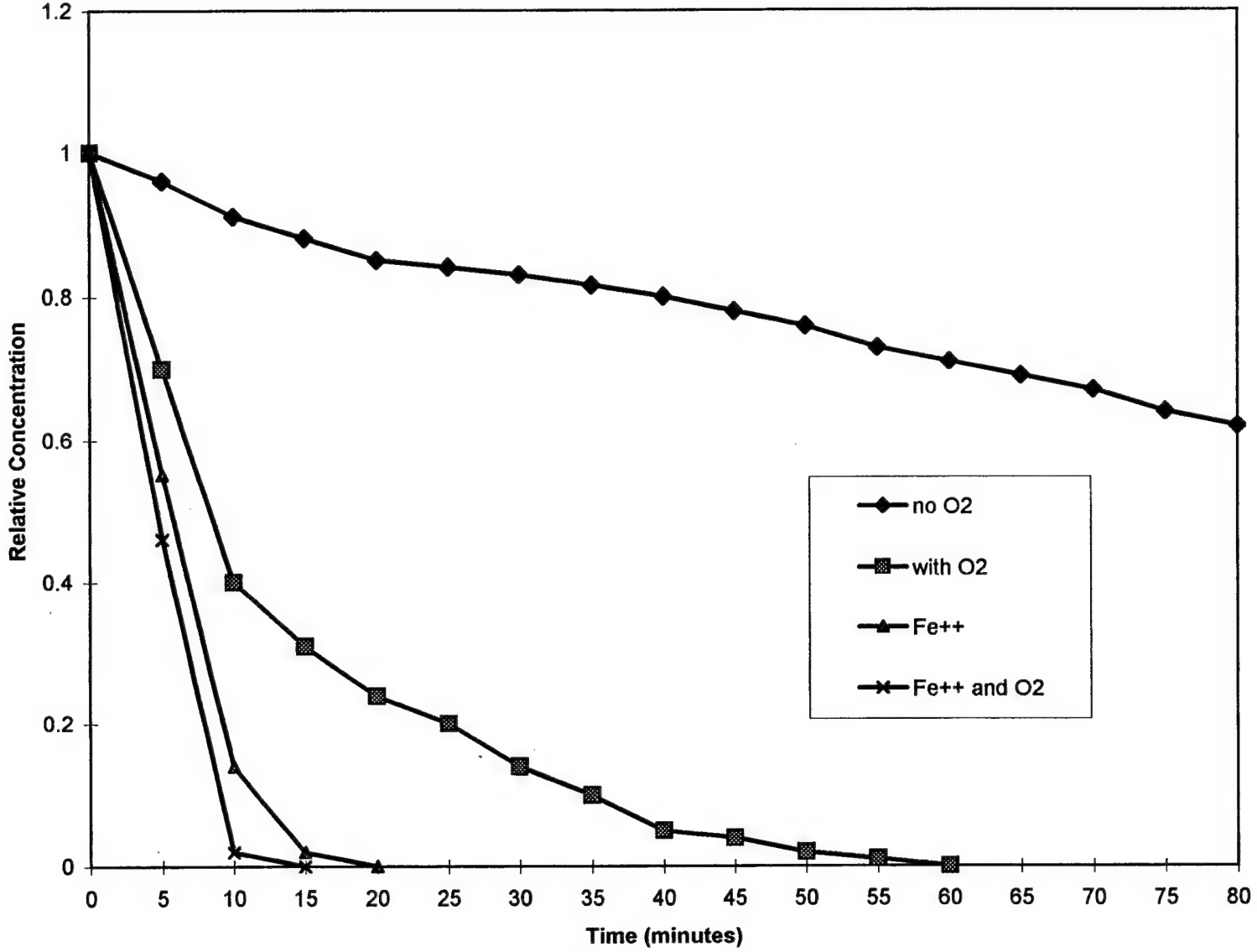

Figure 6 Degradation of Phenol in Florida State University Corona Pulsed Discharge Apparatus

If a pulsed corona discharge system can mineralize phenol, it is believed capable of mineralizing PCBs, since the C-Cl bond strength is about one half the C=C (ring) bond strength.

The data show that corona discharge alone is not very effective in degrading phenol. When oxygen is added, degradation rates increase significantly. The addition of ferrous iron ion improves process effectiveness to an even greater extent. This effect is thought to be due to Fenton's reaction:

$$Fe^{2+} + H_2O_2 \rightarrow \bullet OH + OH^- + Fe^{3+}$$

This observation implies that the pulsed corona discharge process produces significant amounts of hydrogen peroxide. Comparison of the results for the experiments using ferrous iron ion only and ferrous iron ion plus oxygen leads to the observation that the addition of gaseous oxygen may not be required to achieve a high waste destruction rate.

The technical issues related to the pulsed corona discharge process are: (1) can corona discharges effectively generate large numbers of oxidizing species; (2) are the oxidizing species of sufficient strength, concentration, and longevity to mineralize the target material; (3) are the target organic wastes mineralized to a sufficient extent to permit disposal of the part as non-hazardous waste; (4) how much of the oxidizing potential is "wasted" in oxidation of the substrate material; and (5) what is the efficiency of the process in terms of grams of organic material mineralized per unit of electrical power input?

Evaluation of pulsed streaming corona discharge process was planned to proceed by four steps. First, the process variables (such as geometry, pulse width, electrical field strength, etc.) would be optimized through a series of experiments using an organic dye. An organic dye was selected for this step because the process effectiveness can be easily observed and accurately measured. The second step would perform a series of experiments using phenol as the surrogate waste. These experiments would attempt to duplicate the results presented in Reference 2. Third, the degradation of a chlorinated aromatic, such as tetrachlorophenol (a surrogate for PCBs) would be evaluated. Finally, the performance of the process would be evaluated using actual samples of PCB contaminated parts.

RESULTS

Theory

It is helpful to develop some simple models of the corona discharge process to aid in understanding the importance of different variables and as an aid in design of experiments. It is desired to estimate the kinetic energy an electron acquires when accelerated by a high voltage pulse. The kinetic energy is equal to

$$KE = \tfrac{1}{2}\, mV^2, \text{ Joules} \qquad (1)$$

where,

m = mass of an electron, kg
V = velocity, m/sec

The velocity is the integral of the acceleration. For an electron in an electrostatic field, the velocity equals:

$$V = \int \Phi\, q/m, \qquad (2)$$

Where

Φ = electrical field strength, Volts/meter
q = charge on an electron, Coulombs, and
m = mass of an electron, kg.

If it is assumed that the electrical field strength is constant over the small region that an electron traverses, equation (2) can be integrated directly to yield an expression for kinetic energy in terms of electron time-of-flight. However, if equation (2) is integrated a second time, the kinetic energy can be expressed as the distance an electron travels:

$$KE = \Phi\, \lambda\, q\,,$$

where λ is the distance traveled.

A value of λ can be estimated by assuming the distance traveled equals the mean free path (MFP) of an electron, that is, the average distance an electron travels before colliding with another body. The mean free path can be estimated from classical gas dynamics if electrons and gas molecules are assumed to behave as inelastic bodies. In this case, the mean free path of a mixture of elections and gas molecules is

$$MFP = 1 / (\pi \Sigma\, n\, d^2_{ab} \sqrt{1+\overline{(m_a/m_b)}\ }) \qquad (3)$$

where

$d^2_{ab} = [(d_a + d_b)/2]^2$
n = number density of particle a or b,
d = diameter of particle a or b, and
m = mass of particle a or b.

Table 1 Values for Mean Free Path Computation

Particle	Mass, g	Diameter, cm	Number density, $1/cm^3$
nitrogen molecule	4.8 E-23	3.7E-8	2.7E+19
electron	9.11E-28	2.8E-13	1E+13

The value for typical number density of electrons in a non thermal plasma is from Reference (3).

When these values are substituted into equation (3), a value of 3500 E-10 meters (3500 Angstroms) is obtained for the mean free path. The MFP for nitrogen molecules in air at standard conditions is about 654 Angstroms.

Next, the value of electrical field strength, Φ, is estimated. The electrical potential distribution is found by solving Laplace's equation (ref 4):

$$(\nabla^2\Phi) = -q\rho/\varepsilon\,, \quad (4)$$

where

∇ = gradient operator,

Φ = steady state potential,

ε = dielectric constant of the medium,

ρ= charge density.

For cases of interest in this analysis, $\rho = 0$. Therefore,

$$(\nabla^2\Phi) = 0 \quad (5)$$

Equation (5) can be solved for an arbitrary geometry and set of initial conditions using numerical methods. Once the voltage distribution is determined, the gradient can be calculated.

Two dimensional solutions to equation (5) can be calculated using a computer spreadsheet program, such as Microsoft Excel®. The spreadsheet is set up to model the geometry and boundary conditions. The potential at any grid location is equal to the average of the potentials of the surrounding four grid points as calculated using the standard central difference equation. Excel will automatically iterate to a solution. The solution for the potential field of a 0.5mm diameter wire, 3.5 cm long, separated from a plate by a distance of 2.5 cm is shown in Figure 7. In Figures 7 through 9, one unit on plot equals 0.5 mm distance. The wire is charged to +25 kV and the plate to 0 V.

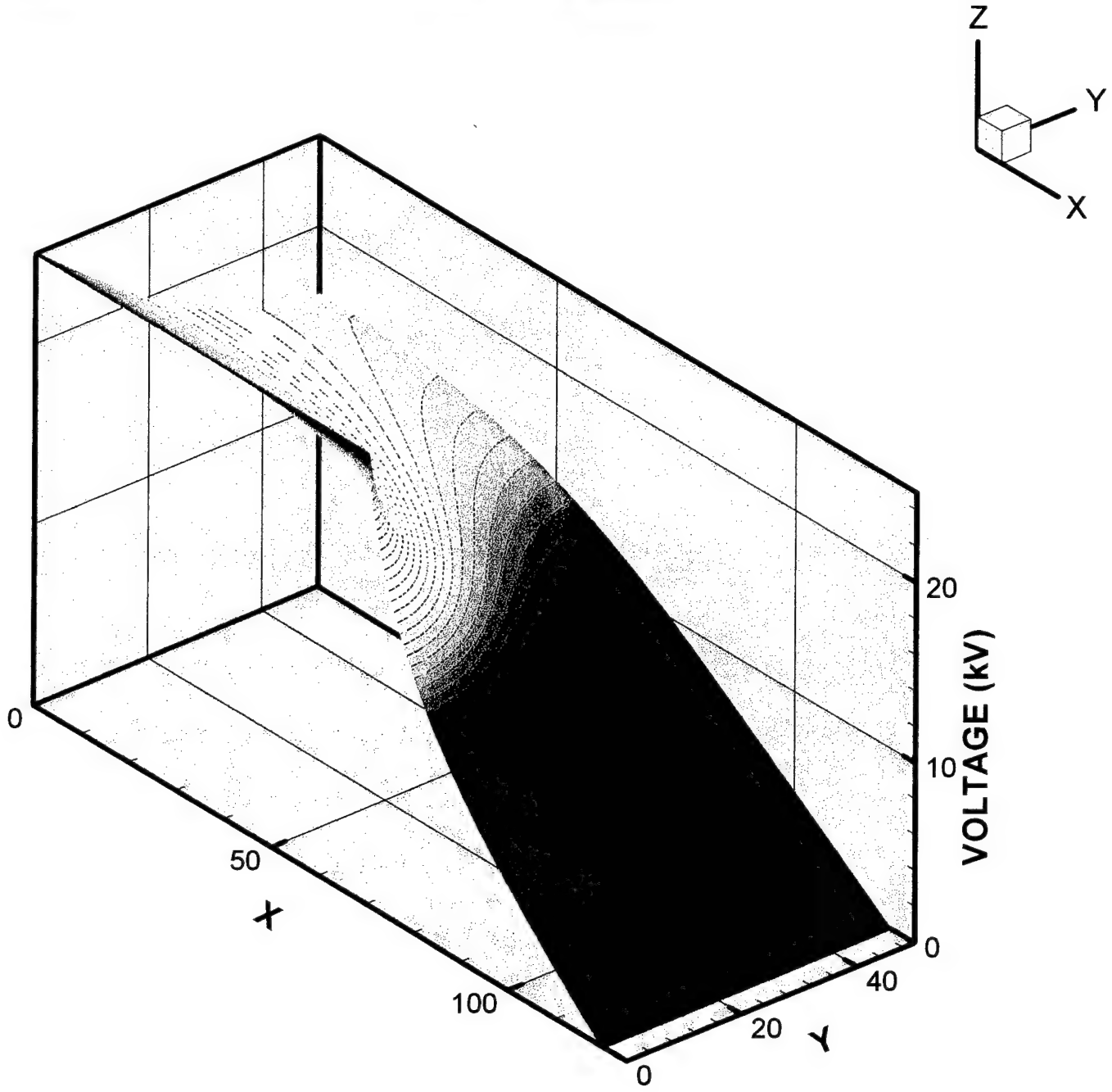

Figure 7 Potential Field for Point and Plane Geometry

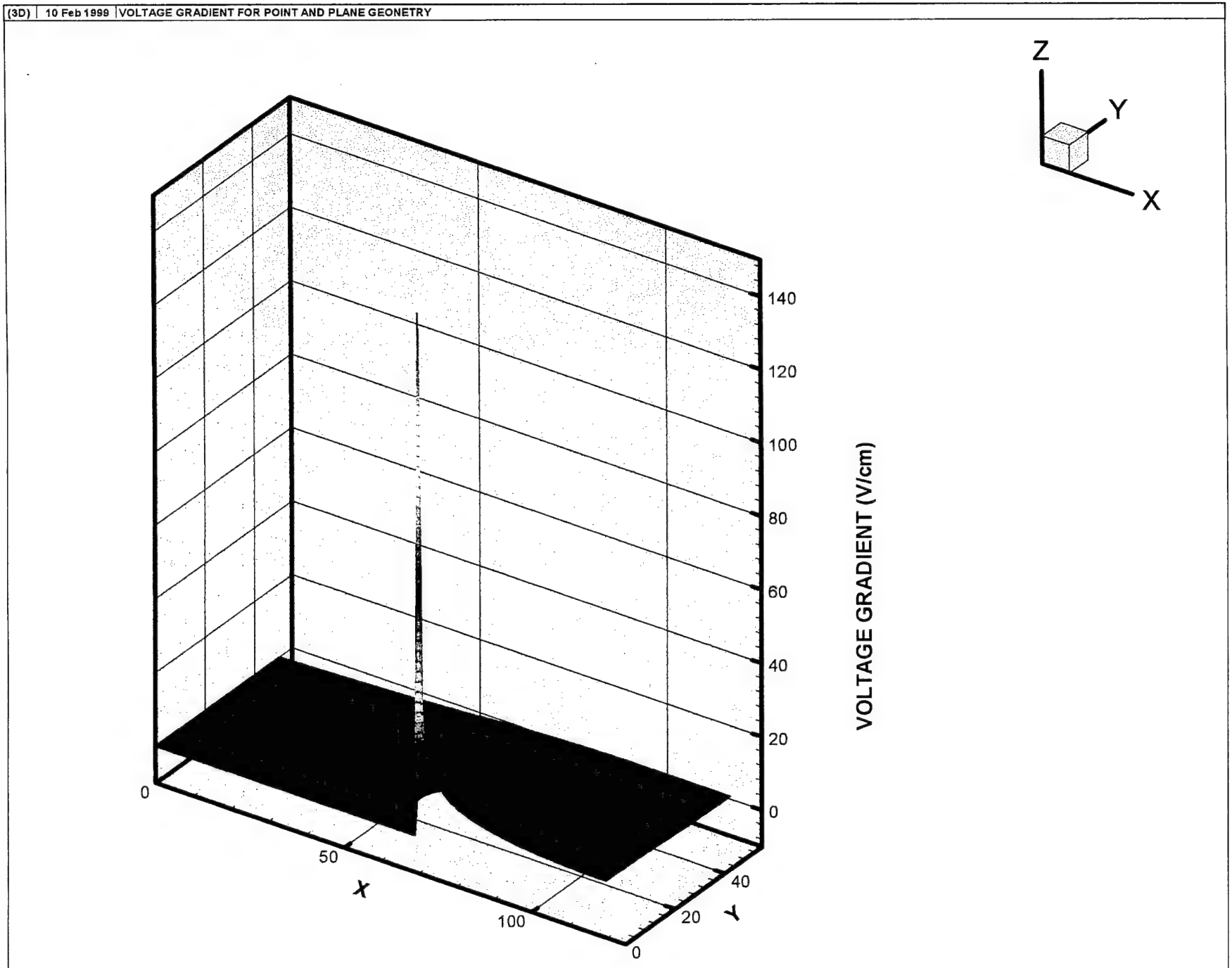

Figure 8 Voltage Gradient for Point and Plane Geometry

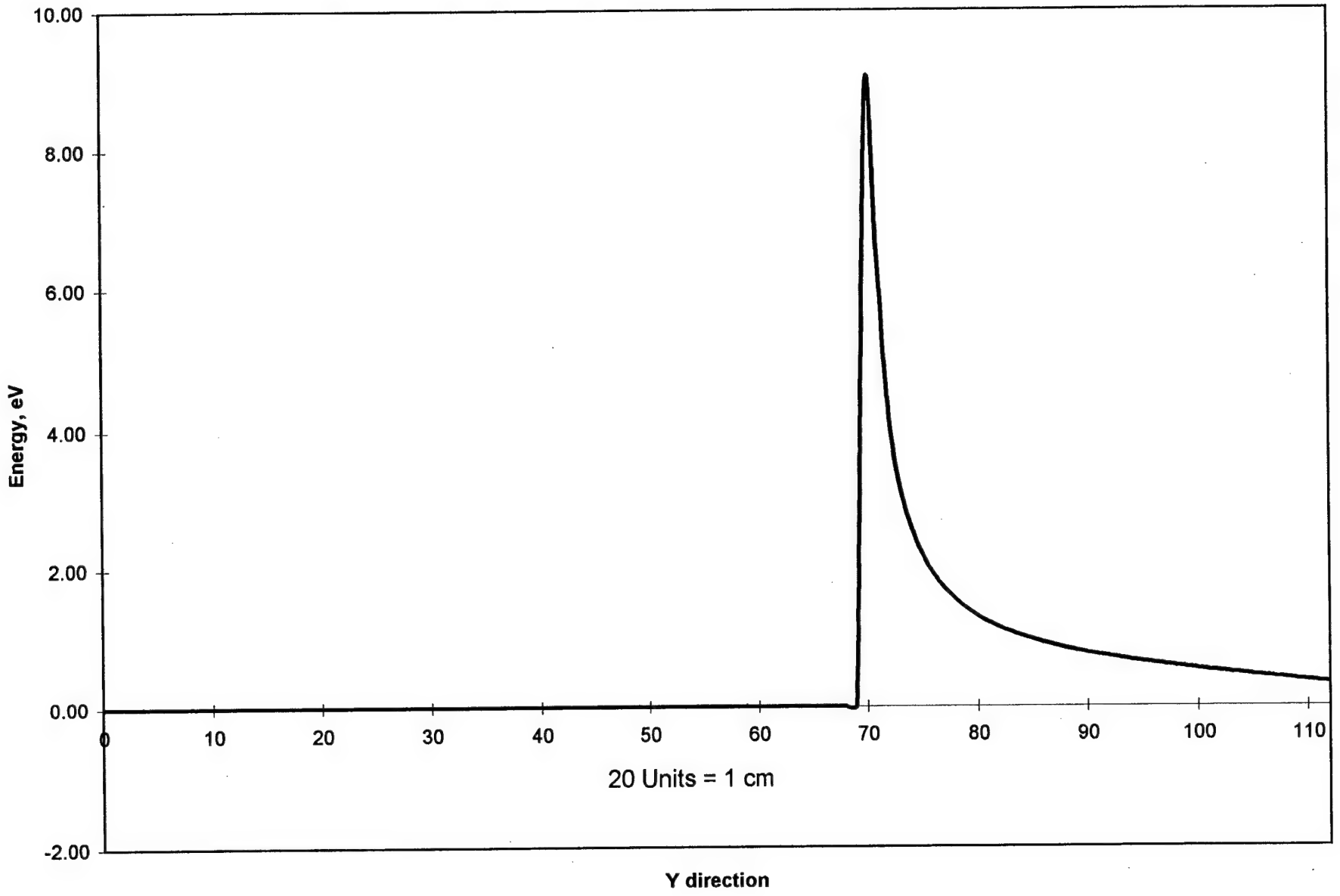

Figure 9. Spatial Distributin of Kinetic Energy Achieved by an Electron (Wire to Plane Geometry)

The difference between the voltage of adjacent cells is the voltage gradient. Of interest in this study is the gradient in the Y direction, i.e., in the direction of the wire tip to the plane. The gradient in the Y direction is shown in Figure 8. Figure 8 shows that a very high potential gradient exists near the very tip of the wire. The magnitude of the gradient for this case is about 130,000 V/cm. This strong localized electric field accelerates electrons to high energy levels.

Knowledge of the spatial distribution of electrical field strength and the mean free path permits calculation of the distribution of kinetic energy. The result is presented in Figure 9. Figure 9 shows that energy levels in excess of 8 eV can be achieved with the wire and plane geometry. As Figure 9 shows, the region of energetic electrons is small. The volume of the active processing region near the tip of the wire is perhaps one cubic millimeter.

The results presented in Figure 9 can be compared to results predicted by very detailed models developed by Lawrence Livermore National Laboratory (Figure 10, from Ref. 5). Both models predict electron energy levels of about 8-10 eV for a field strength of 130 kV/cm.

Figures 11, 12, and 13 show results for another geometry of interest: a wire along the axis of a cylinder. The concentric cylinder geometry is one of the few geometries that have a closed form solution of Laplace's equation. The solution is

$$\Phi_{max} = \Phi / r_a \ln(r_b/r_a) \qquad (6)$$

where

Φ_{max} = potential at the surface of the inner cylinder

Φ = potential difference between the inner and outer cylinders

r_a = radius of inner cylinder

r_b = radius of outer cylinder.

The results computed by the spreadsheet based finite difference method are within 0.1% of the exact solution for the cylinder-in-cylinder geometry.

The finite difference code for calculating the potential gradient was used to estimate the affects of geometry, applied voltage, and polarity.

The kinetic energy achieved by an electron in a pulsed corona generator can be compared to the bond energy of some common organic chemicals.

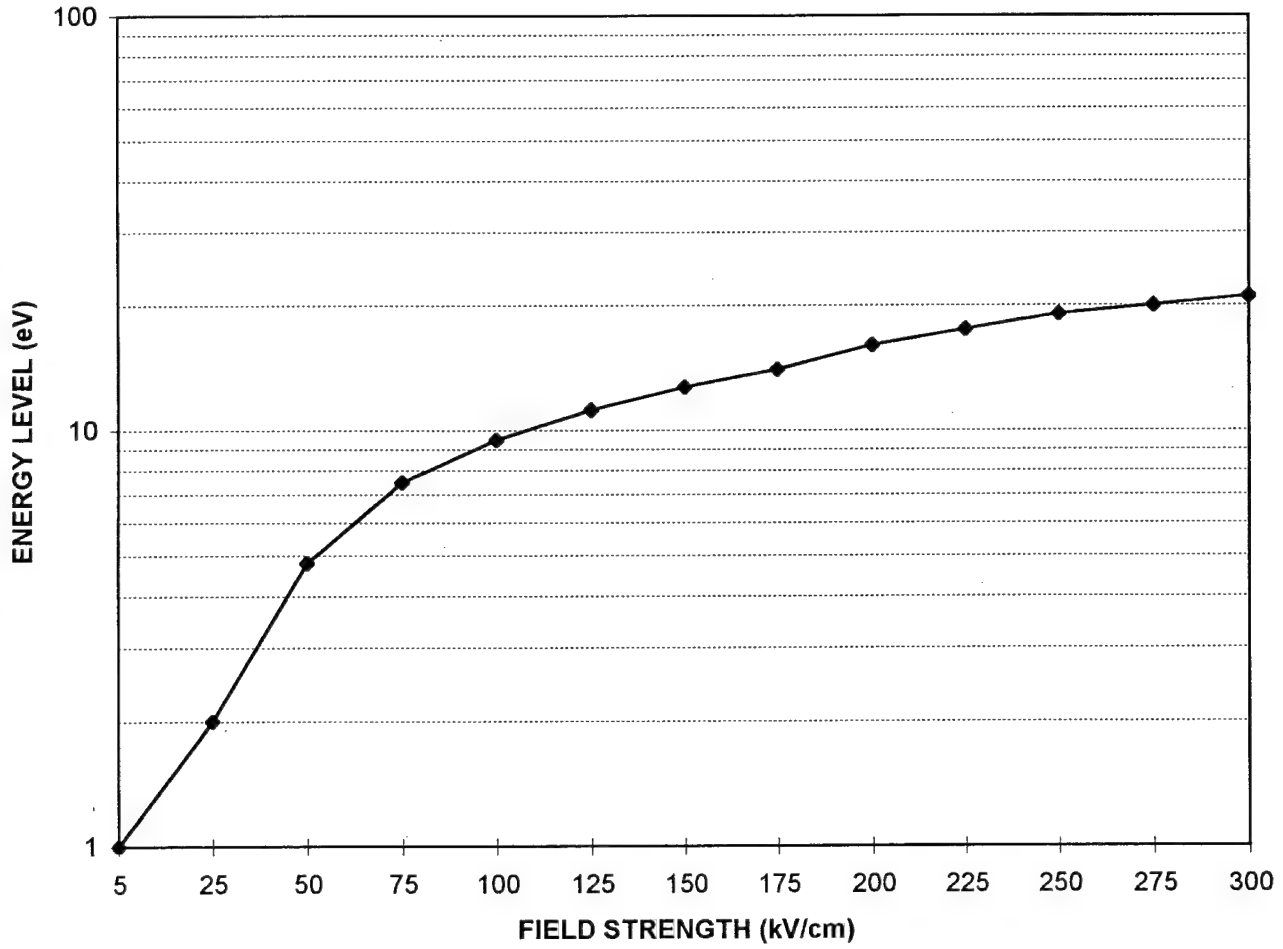

Figure 10 Electron Energy Level Versus Field Strength (from Ref. 5)

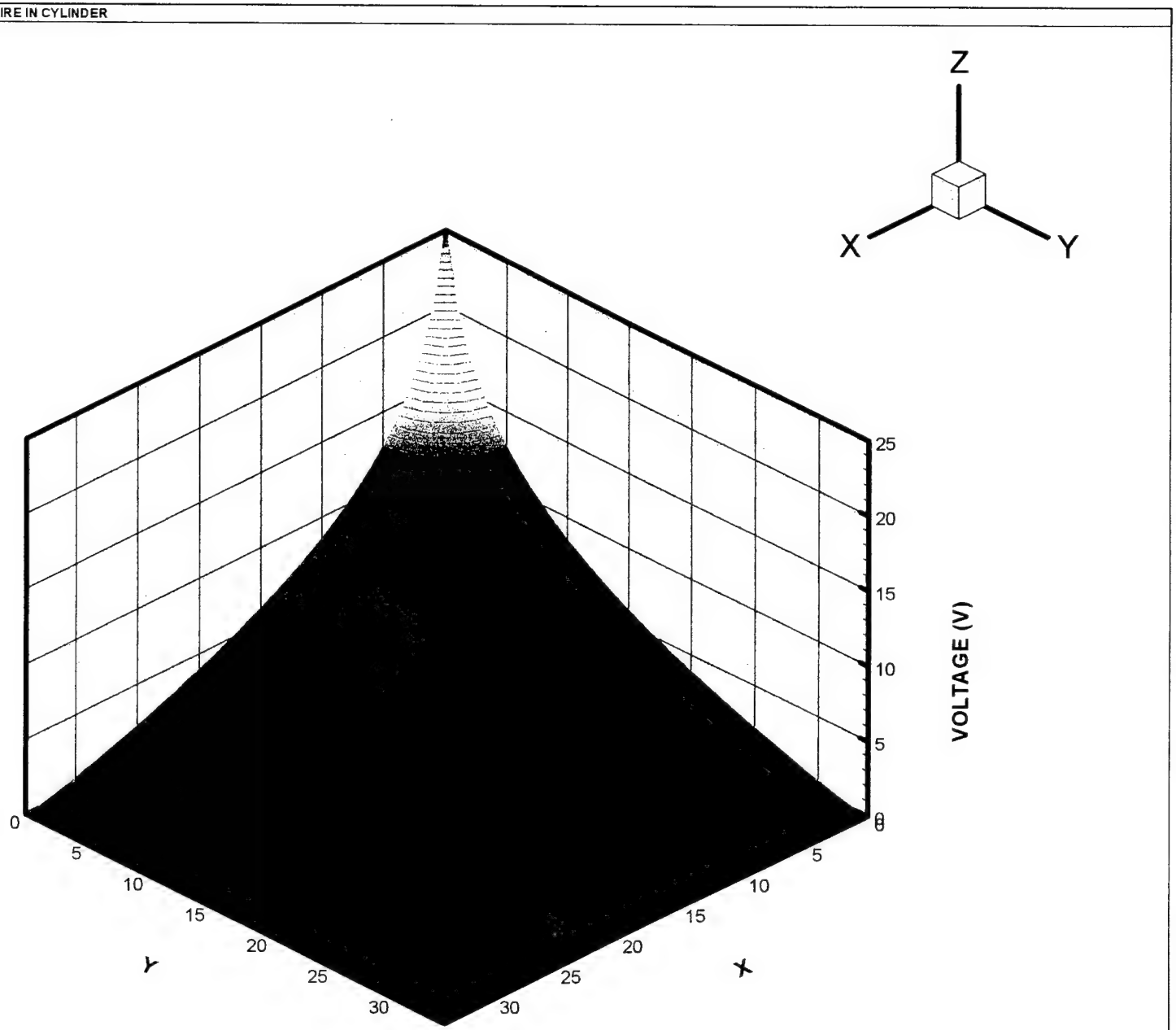

Figure 11 Potential Field for Wire-in-Cylinder Geometry

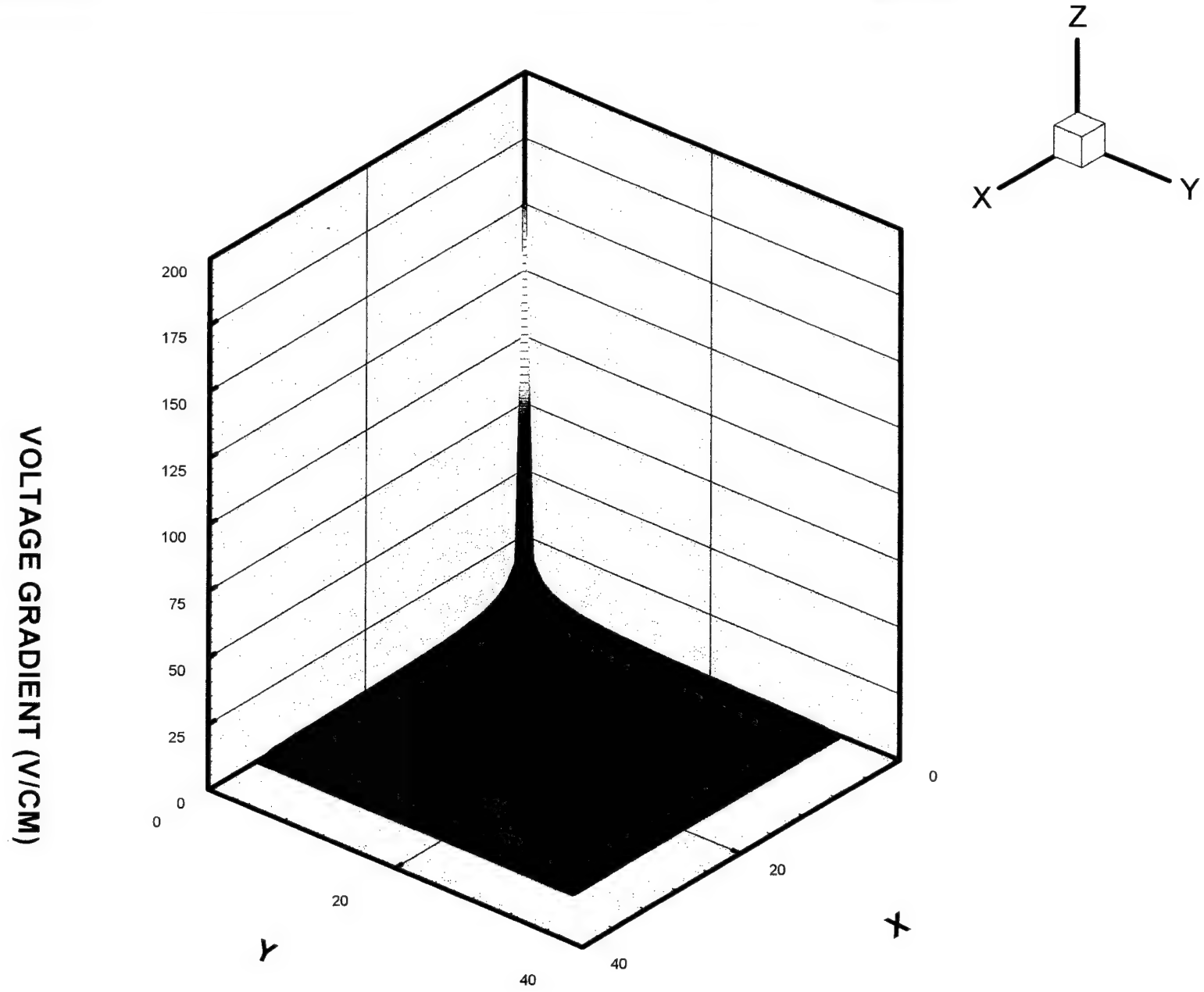

Figure 12 Field Gradient for Wire-in-Cylinder Geometry

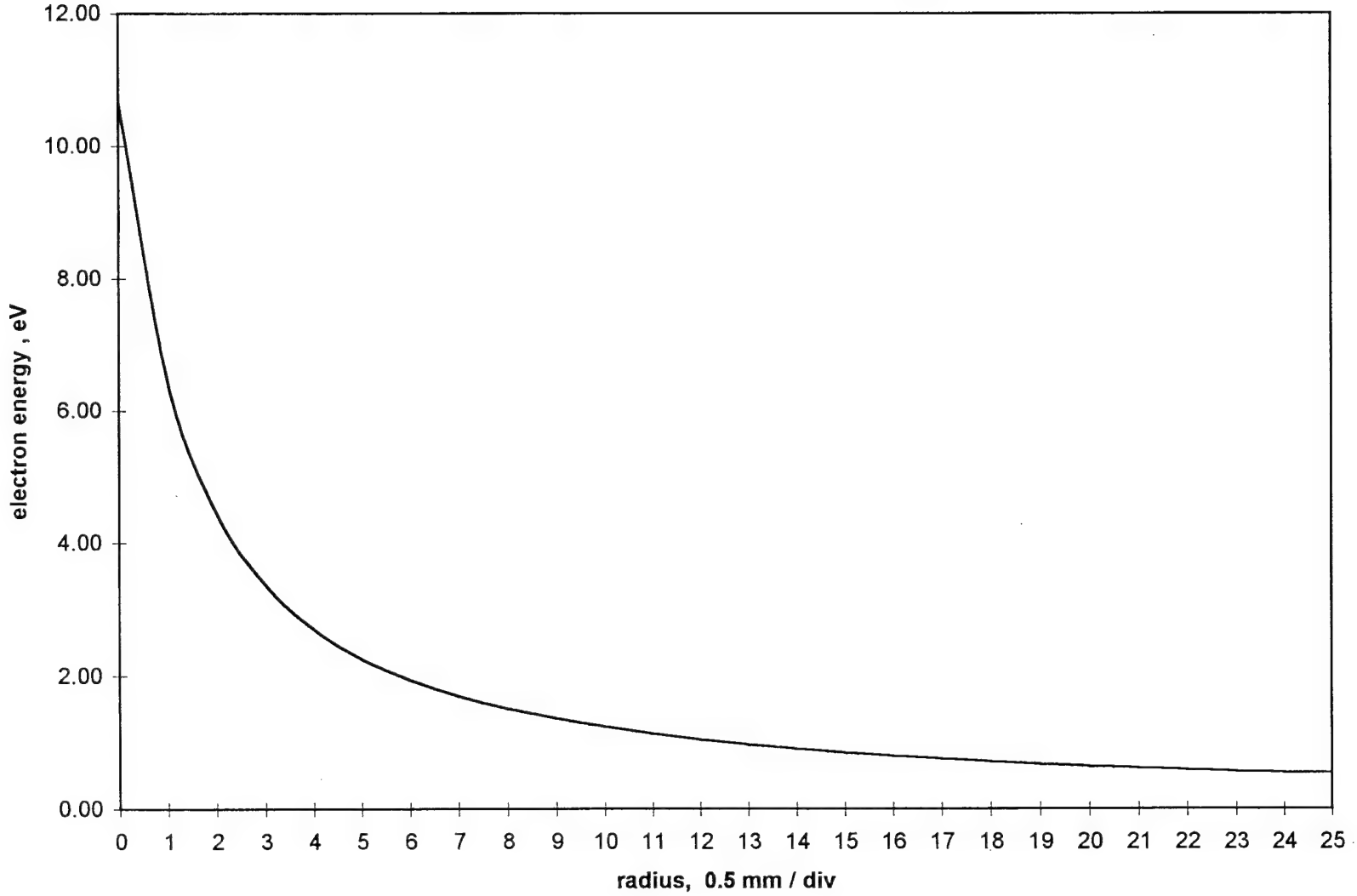

Figure 13. Electron Energy Versus Radius

Table 2. Bond Energy, eV (Reference 6)

C-C	3.6	C=C	6.3
C=C (in a ring)	5.5	C-H	4.3
C-O	3.7	C=O	7.7
C=O (in a ring)	8.3	C-Cl	3.5
O-O	1.5	O-H	4.8
C-C (in a ring)	5.3	H-Cl	4.4
Cl-Cl	2.5	N-H	4.0

The data in Table 2 indicate that it may be possible to break several types of organic molecules bonds by direct bond scission with 8 to10 eV. Of special interest are the C=C bond (in a ring), the C-C bond (in a ring) and the C-Cl bond. These types of bonds are found in PCBs.

Experiment

Apparatus. A schematic of the experimental apparatus is presented in Figure 14. A clear acrylic reactor vessel rests on a magnetic stirrer base. The volume of the vessel is approximately 1 liter. The bottom of the reactor vessel is covered with a brass plate that serves as one electrode. The top of the reactor vessel houses an insulated hollow electrode that terminates in a very fine (0.022 in. outside diameter) stainless steel tube honed to a sharp tip. The distance between the hollow electrode and the planar electrode can be adjusted to change the value of electrical field strength. A gas, such as air or oxygen, can be introduced into the reactor vessel through the tip of the tubular electrode. The top of the reactor vessel also contains connections to a gas sampling system. Liquid from the reactor vessel is circulated by a small pump through a cuvette and returned to the reactor vessel. A collimated beam of light passes through the cuvette and is focused on one end of a fiber optic cable. The other end of the fiber optic is connected to spectrophotometer. A diffraction grating in the spectrophotometer spreads the beam of light across a linear array of photodiodes. The spectrophotometer measures and records the absorption spectrum in the visible range, i.e., for wavelengths from about 400 nm to 800 nm. The spectrophotometer was used to measure changes in composition of organic dyes. Kinetics data are obtained by using the spectrophotometer to measure and record the absorption at a specific wavelength over a period of time. The preliminary process sensitivity studies were accomplished by measuring the absorption of acid blue 40 dye at its peak absorption frequency over a period of 15 minutes.

A pulse power generator supplies electrical input to the apparatus. The power supply was custom designed and built by Integrated Applied Physics, Inc. of Pasadena, CA. A schematic of the pulse generator is presented in Figure 15. The pulse generator consists of a high voltage direct current power supply, a very rapid switch, and a pulse-forming network. The power supply is a commercially available 30 kV, 1.5 kW DC unit. Power from the DC source is switched into the pulse-forming network with a special high voltage vacuum tube switch. The pulse forming network consists of a series of inductors and capacitors connected together to form a discrete delay line. The baseline pulse-forming network consists of 8 elements, giving a total pulse width of $8\sqrt{LC}$, where L is

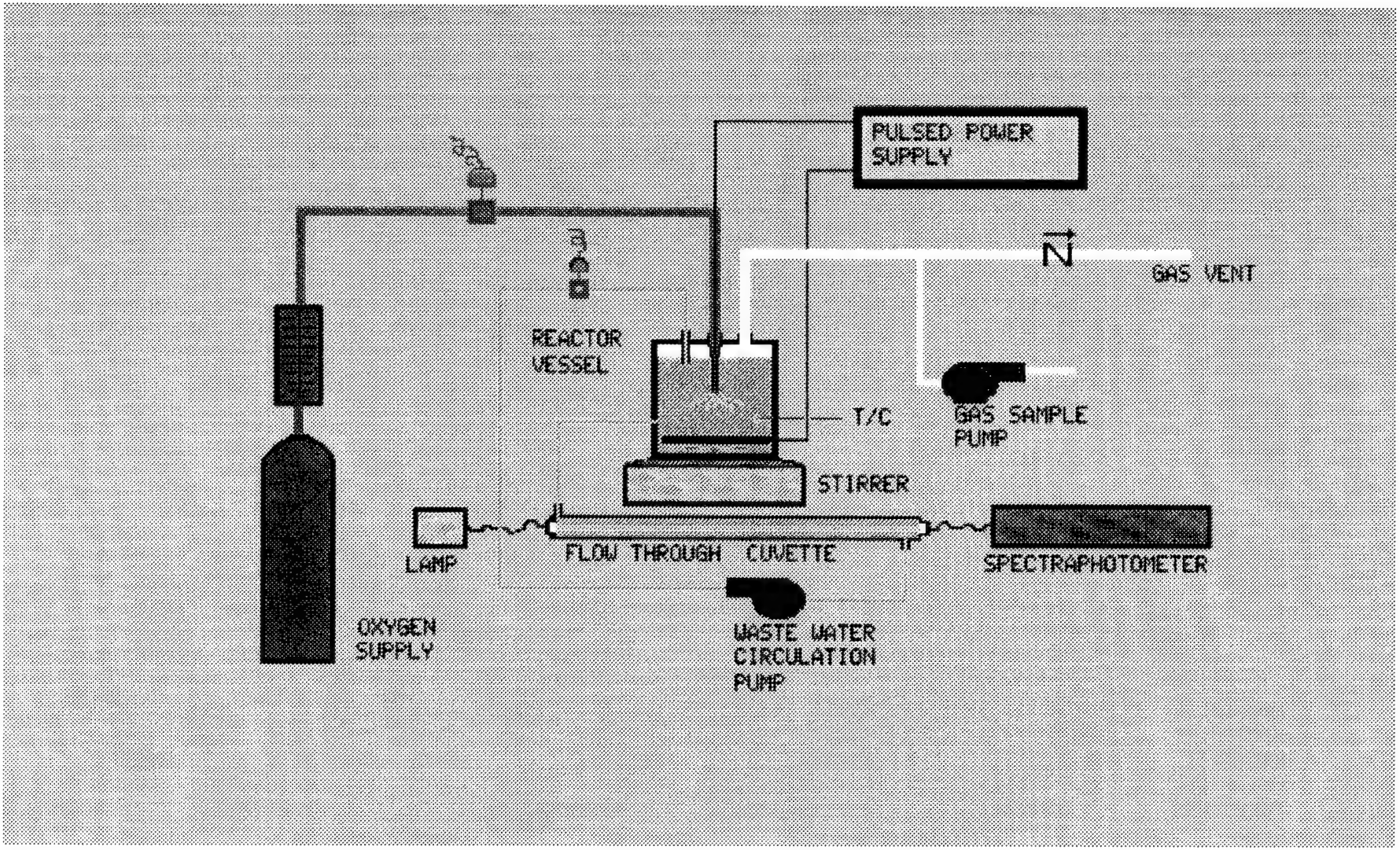

Figure 14 Schematic of Experimental Apparatus

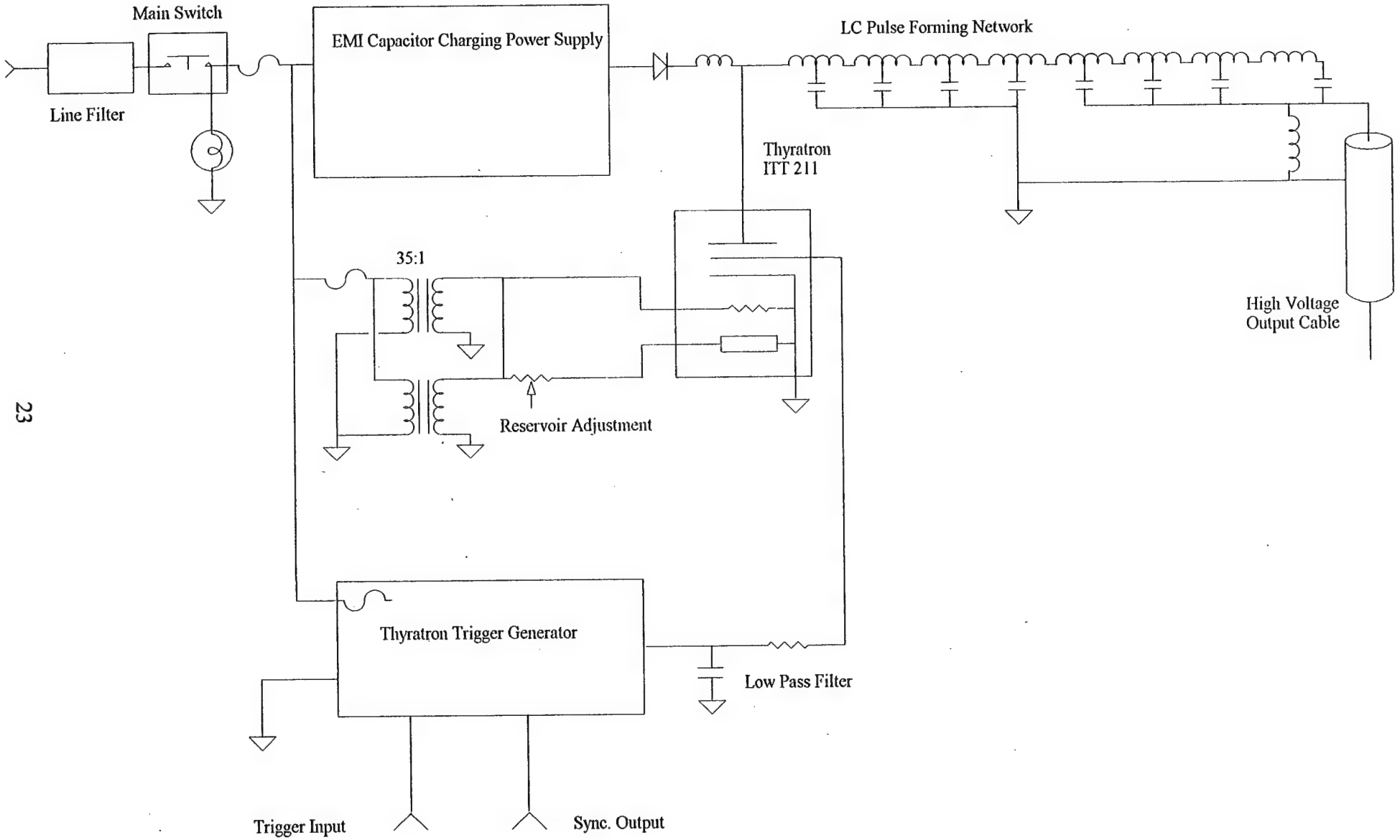

Figure 15. Schematic of Pulsed Power Generator

the element inductance in Henrys and C is the element capacitance in Farads. Values of L = 0.4 μ H and C = 100 pF yield a baseline pulse duration of 50 x 10^{-9} seconds. Other values of pulse duration are achieved by changing values of L and C. The pulse frequency is variable from about 20 Hz to 1 kHz. Output voltage is adjustable from 0V to about 35 kV. Frequency and voltage are adjustable by dials on the front panel of the power supply.

The voltage across the load is measured with a Tektronix Model P6015A high voltage probe. This probe has a 1000 X attenuation. Current flow through the test cell is measured with a current viewing resistor from T&M Research Products Inc., Albuquerque, NM. A current viewing resistor outputs a voltage proportional to the current flowing through the circuit. Voltages and waveforms are measured and recorded with Tektronix Model 2430 digital oscilloscope. Knowledge of the voltage and current waveforms permits calculation of the power consumed by the process.

Changes in the absorption characteristic of a target chemical compound can be correlated with changes in concentration of the chemical. The change in concentration, together with knowledge of the power consumed in the process, permit computation of the power required to treat a mole of the target compound. Process efficiency is measured in terms of moles of hazardous material mineralized per watt-hr input.

Experiments were conducted to match the impedance of the load (the reactor vessel) to the impedance of the pulse generator. Maximum power is transferred from the power supply to the reactor when the impedance of the reactor equals that of the pulse generator. An approximate impedance match occurs when the charging voltage on the pulse generator network is equal to the voltage difference across the load and the pulse waveform is critically damped. In some experiments, resistors were connected in parallel to the reactor vessel to match the load impedance to the pulse generator impedance. The resistors are 100 W, non-inductive devices obtained from Hipotronics Corp., Brewster, NY. In other experiments, changing the conductivity of the solution was used to vary the load impedance.

The experimental apparatus was monitored and controlled by a mouse-actuated graphical computer interface based on analog-to-digital computer boards and software drivers from National Instruments, Inc., Austin, TX. The system provided data monitoring and acquisition capabilities as well as the ability to remotely turn equipment items on and off. The graphic presented in Figure 14 is a screen graphic from the control program.

Photographs of the experimental apparatus are presented in Figures 16 and 17.

A photograph of a typical corona discharge is presented in Figure 18. The corona discharge consists of a central spot, bright white in color, surrounded by magenta colored filaments. The magenta color of the filaments has been attributed to the Balmer series of emission lines from gaseous atomic hydrogen (Reference 6). Corona streamer length is observed to be a function of potential difference, solution conductivity, and reactor geometry. Long corona streamers are produced by a combination of high potential difference, low solution conductivity, and small electrode areas. Typical streamer lengths

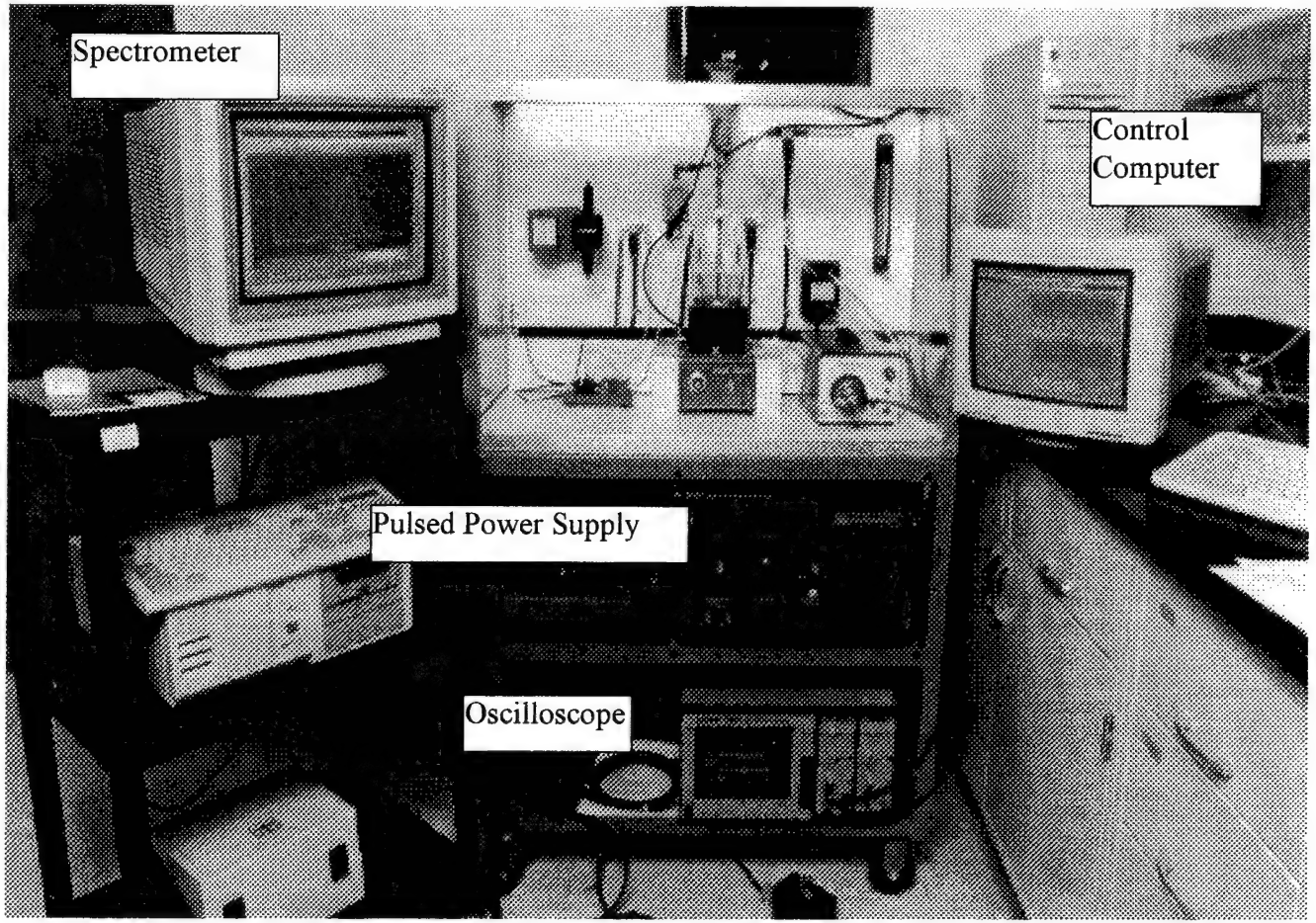

Figure 16. View of Experimental Apparatus

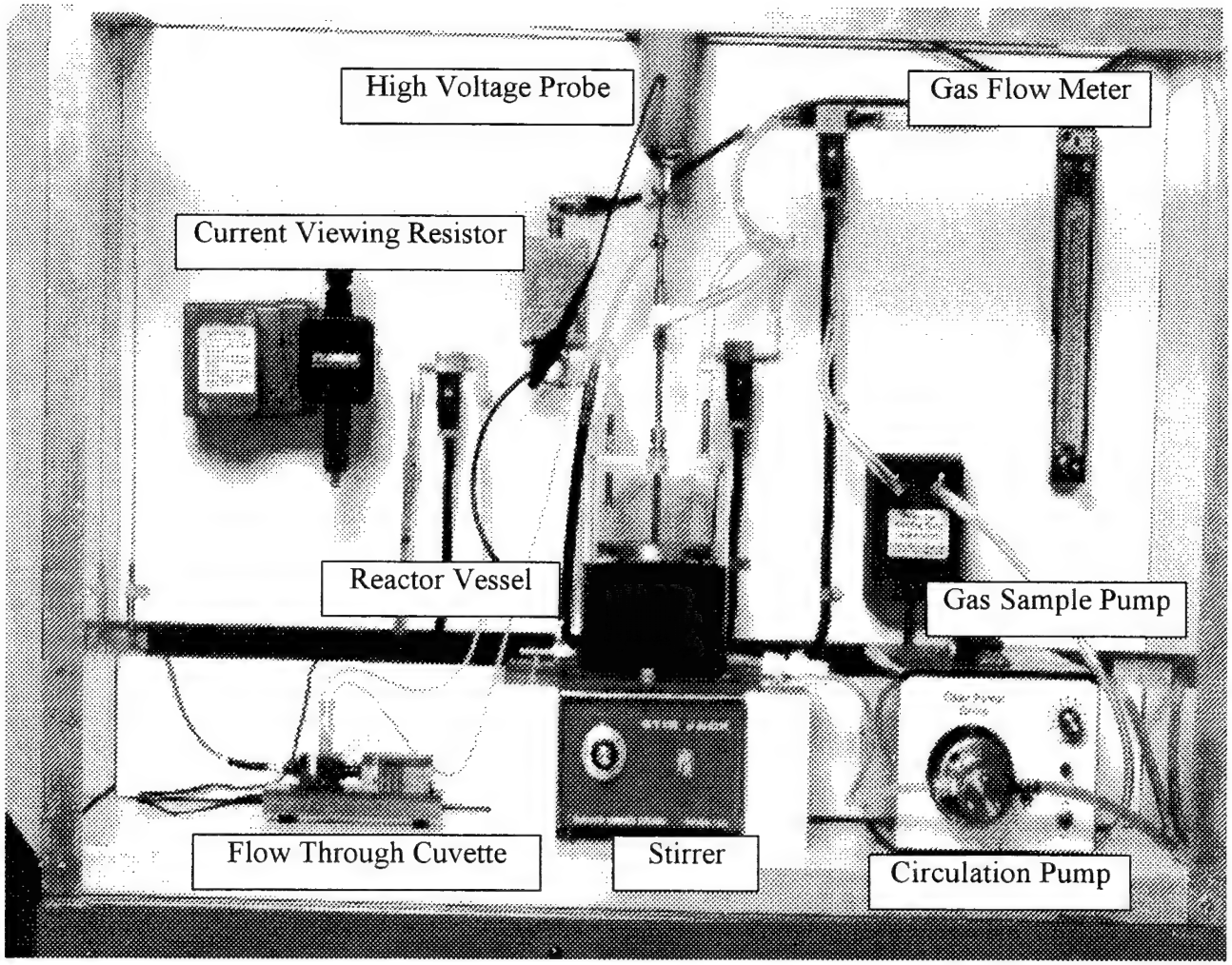

Figure 17 Close View of Experimental Apparatus

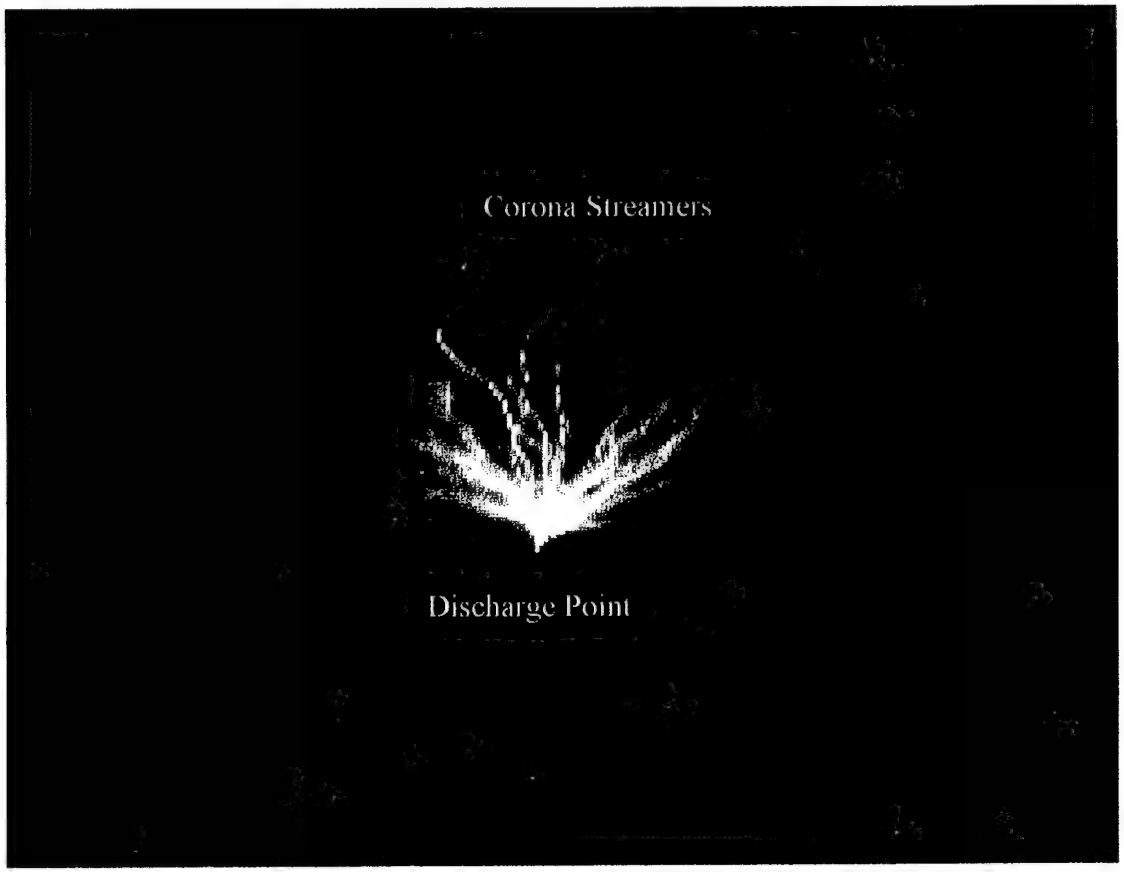

Figure 18. Pulsed Corona Discharge

(in de-ionized water with 25 kV) are 2.5 to 3 cm. Occasionally, a corona streamer will be long enough to touch the grounded electrode. When this occurs, there is an immediate direct discharge, or spark-over. The streamer is converted into a high-current arc that emits a very bright white light and is accompanied by a loud "crack" sound. Voltages greater than 35 kV consistently produced spark-over with 5 cm electrode separation.

Results

Dye de-coloration studies. The goal of the first series of experiments was to identify the most important variables for a pulsed plasma corona discharge apparatus, i.e., separate the important variables from those having a second order or no effect on the result of the process. Table 3 presents a list of known process variables.

Table 3. Pulsed Corona Discharge Process Variables

Variable	Range of values
Electrical Field Strength	6 kV/cm to 10 kV/cm average field strength
Pulse Repetition Rate	50 Hz to 1 KHz
Pulse Duration	50 ns to 1500 ns
Pulse Polarity	Positive or negative
Geometry	Single or multiple discharge points
Gas Flow Rate	0 to 150 ml/min
Gas Composition	Argon, oxygen or air
Fluid pH	4, 7, and 10 pH
Fluid Conductivity	1μ Mhos/cm to 50,000 μ Mhos/cm
Catalysts and co-reactants	Ferrous iron, titanium dioxide
Buffers	Phosphate, borate

Figure 19 shows the basic absorption spectrum of a 1.0×10^{-4} concentration of the organic dye, acid blue 40. The structure of acid blue 40 consists of 4 interconnected benzene rings with 3 oxygen atoms, 1 carbon atom, 3 amine molecules, 1 sodium sulfate molecule, and 1 methane molecule attached at various points on the rings. Figure 20 presents the correlation between molarity and absorption.

Case 1. Baseline Performance. Figure 21 presents several measures of baseline performance. As the data show, when the solution is simply circulated through the cuvette, the concentration of the acid blue 40 dye does not change. The data also show that the dye does not oxidize when air or oxygen is simply bubbled through the solution.

Case 2. Gas Flow Rate. Figure 22 shows the sensitivity of process performance to the flow rate of gas through the needle electrode. Within experimental error, no oxidation of the dye occurs if no gas flows through the needle electrode. It was observed that as the gas flow is decreased, the size and intensity of the plasma discharges decreased, becoming weak and intermittent when the gas flow was reduced to zero. Theory predicts these results. The mean free path of an electron in water is very small, so the kinetic energy of the electrons leaving the needle tip will be very low. There is, however, a

significant change in composition when a high volume (e.g. 150 ml/min) of air flows through the electrode

Case 3. Gas Composition. Figure 23 shows the sensitivity of process performance to composition of the gas flowing through the hollow electrode. These data show that oxygen has a strong effect on system performance, producing an approximately 40 % decrease in the concentration of acid blue 40 over a 15 minute period. Air produces a decrease of about 10 % over the same period. (This reduction in performance is approximately the same as the proportion of oxygen in air). This would indicate that oxygen plays a very important role in the process. This assumption is confirmed by flowing argon through the needle tip. Within experimental error, nothing happens if argon is flowed through the hollow electrode. If the mechanism of pulsed corona discharge works as postulated, some dissociation of organic molecules should due to direct bond scission, regardless of the composition of the gas. This result suggests that direct bond scission by energetic electrons does not play a major role in the process. This result could also be attributed to the fact that the concentration of dye molecules is very low, so the probability of an energetic electron striking a dye molecule is very low.

Case 5. Electrical Field Strength. The effect of changing the electrical field strength is presented in Figure 24. Data are presented in terms of the average field strength: the applied voltage divided by the distance between the two electrodes. In this experimental device, the electrode spacing was 2.5 cm. The data show that the decomposition rate of acid blue 40 increases as the field strength is increased. This result is consistent with theory that predicts higher electron kinetic energy as the field strength is increased.

Case 6. Pulse Rate. Figure 25 shows the effect of increasing the rate at which electrical discharges are produced. Figure 25 shows that increasing the pulse rate increases the rate of change of dye decomposition. This result is expected, since increasing the pulse rate increases the rate at which electrical power is input to the system.

Case 7. Pulse Duration. Initial studies of the effect of pulse duration were not conducted because delays in delivery of the circuit elements required to change the duration of the pulses.

Case 8. Pulse Polarity. The effect of changing the polarity of the pulses is shown in Figure 26. The IAP Inc. power supply delivers a pulse that is negative relative to ground. The term "negative polarity" means that the hollow electrode is briefly at a negative voltage relative to the ground plane when a pulse is delivered. Figure 26 shows that when the output cables of the power supply are reversed (i.e. the wire electrode is briefly at a higher voltage relative to the ground plane), the decomposition rate of the dye is greatly reduced. The mathematical model predicts this result. If the mathematical model is run with reversed polarity, the estimated maximum electron energy level is only about half that for the negative polarity case, i.e. only about 4 eV.

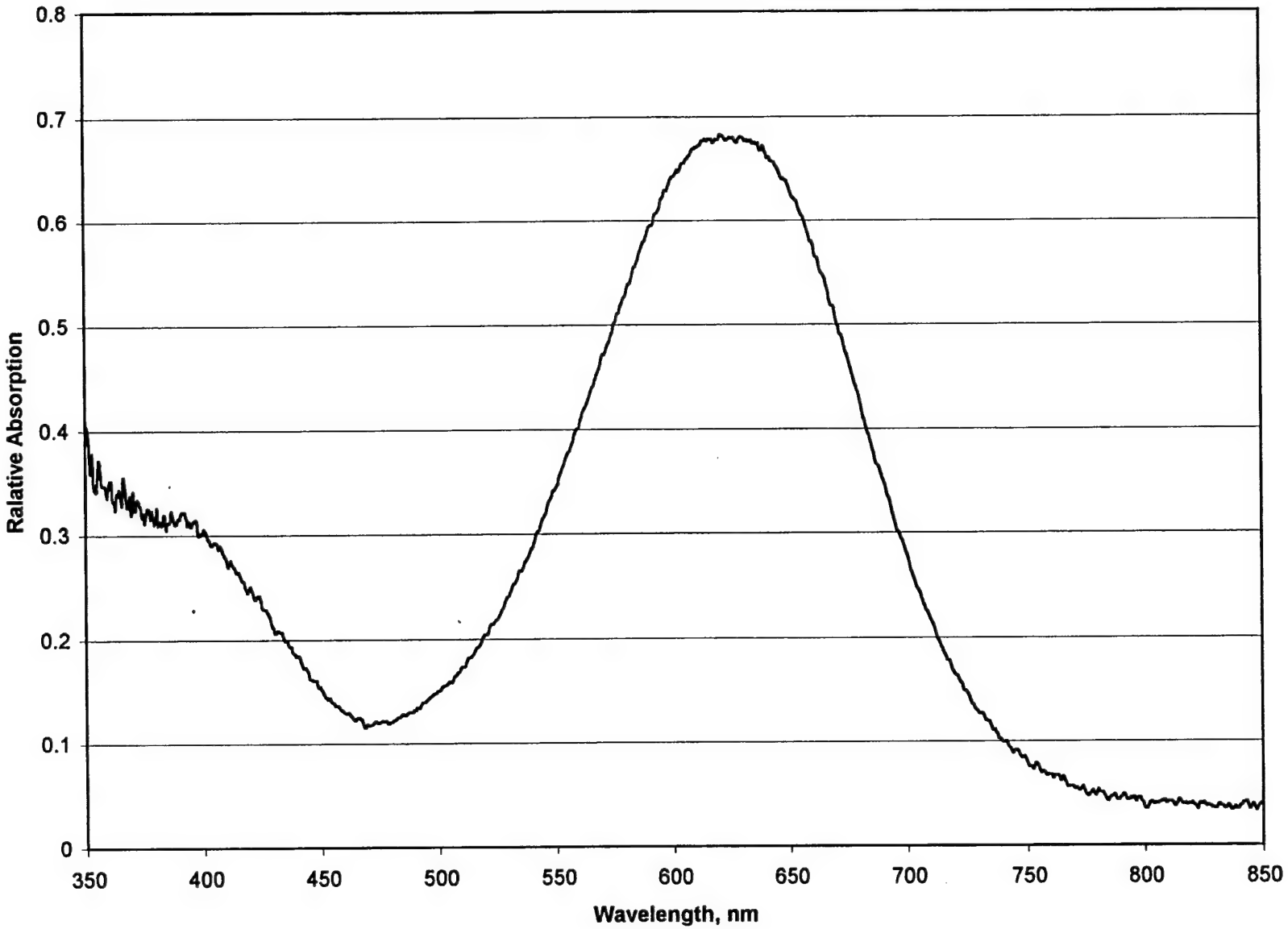

Figure 19 Absorption spectrum for Acid Blue 40 Dye

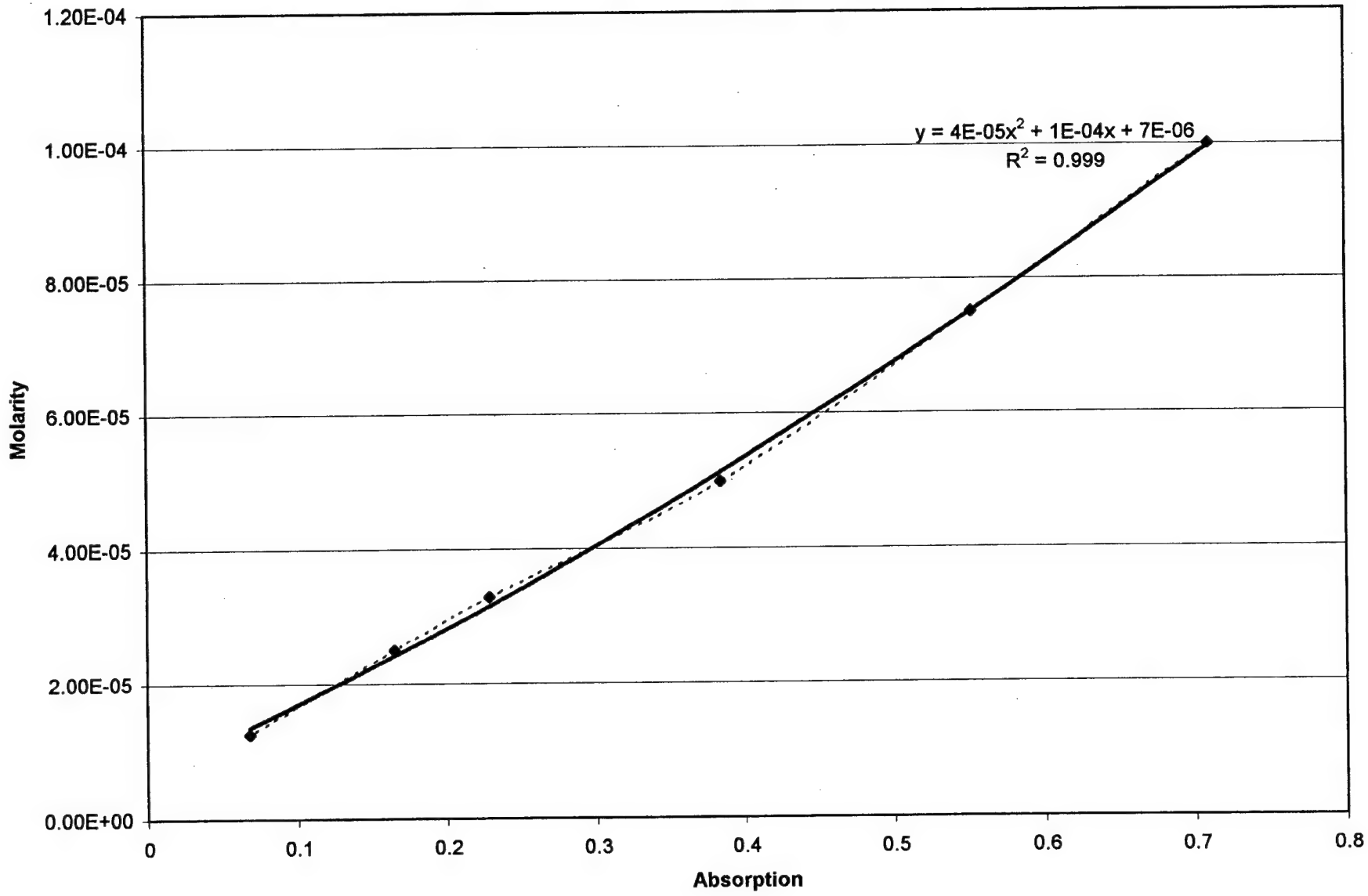

Figure 20. Correlation Between Absorption and Concentration

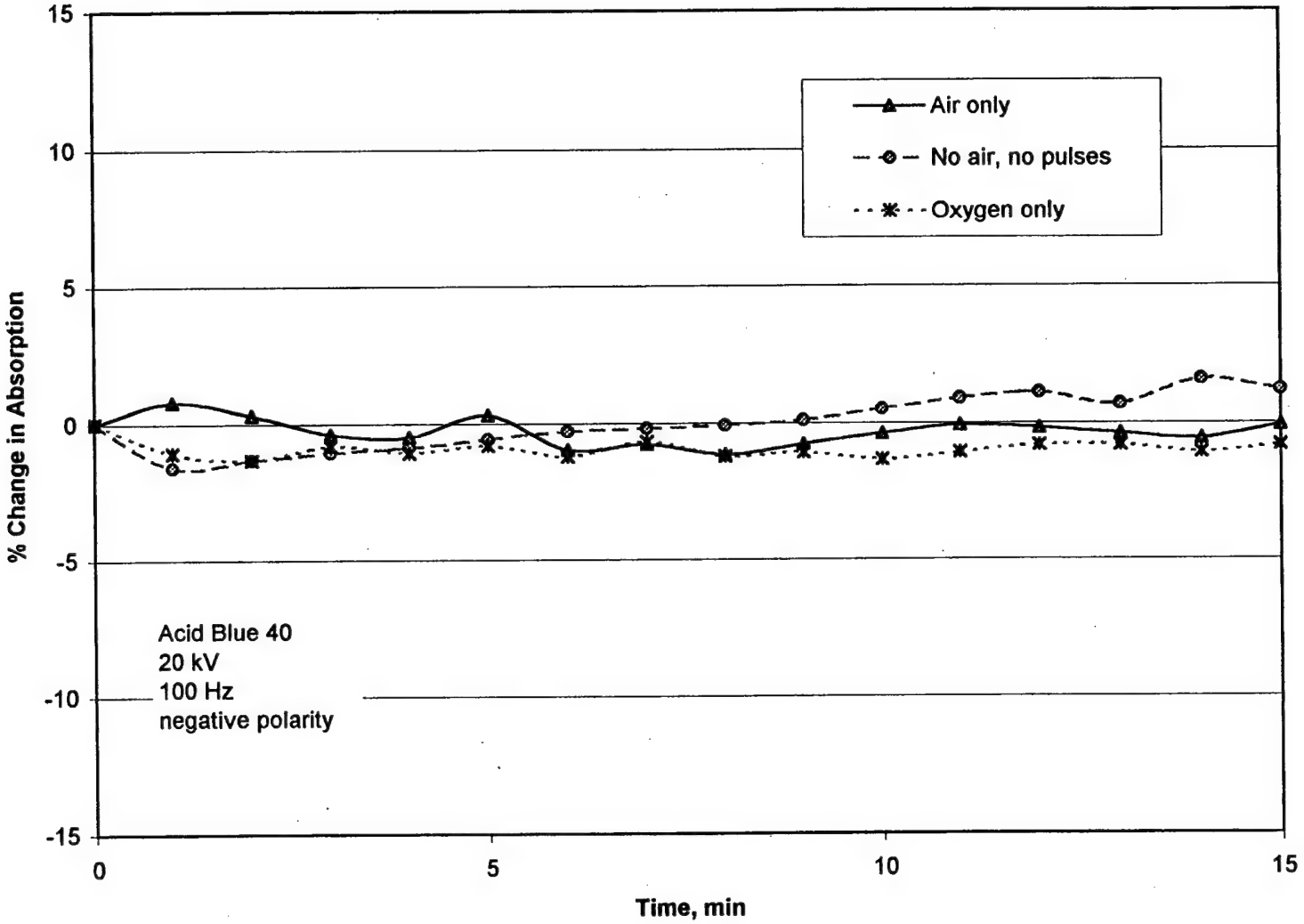

Figure 21 Baseline Performance with Acid Blue 40 Dye

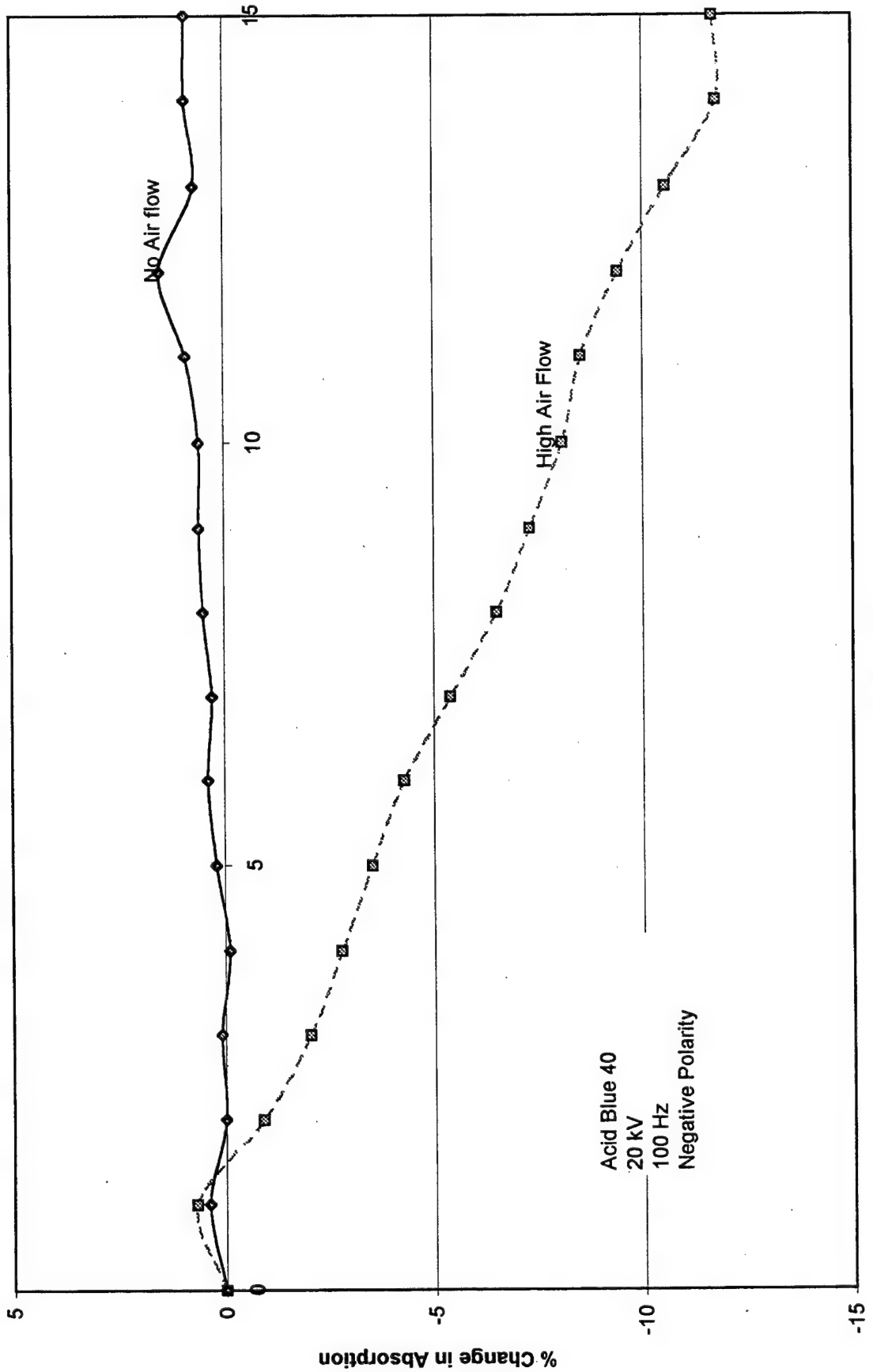

Figure 22 Air Flow Rate Sensitivity

Excel/plasma/bludat26

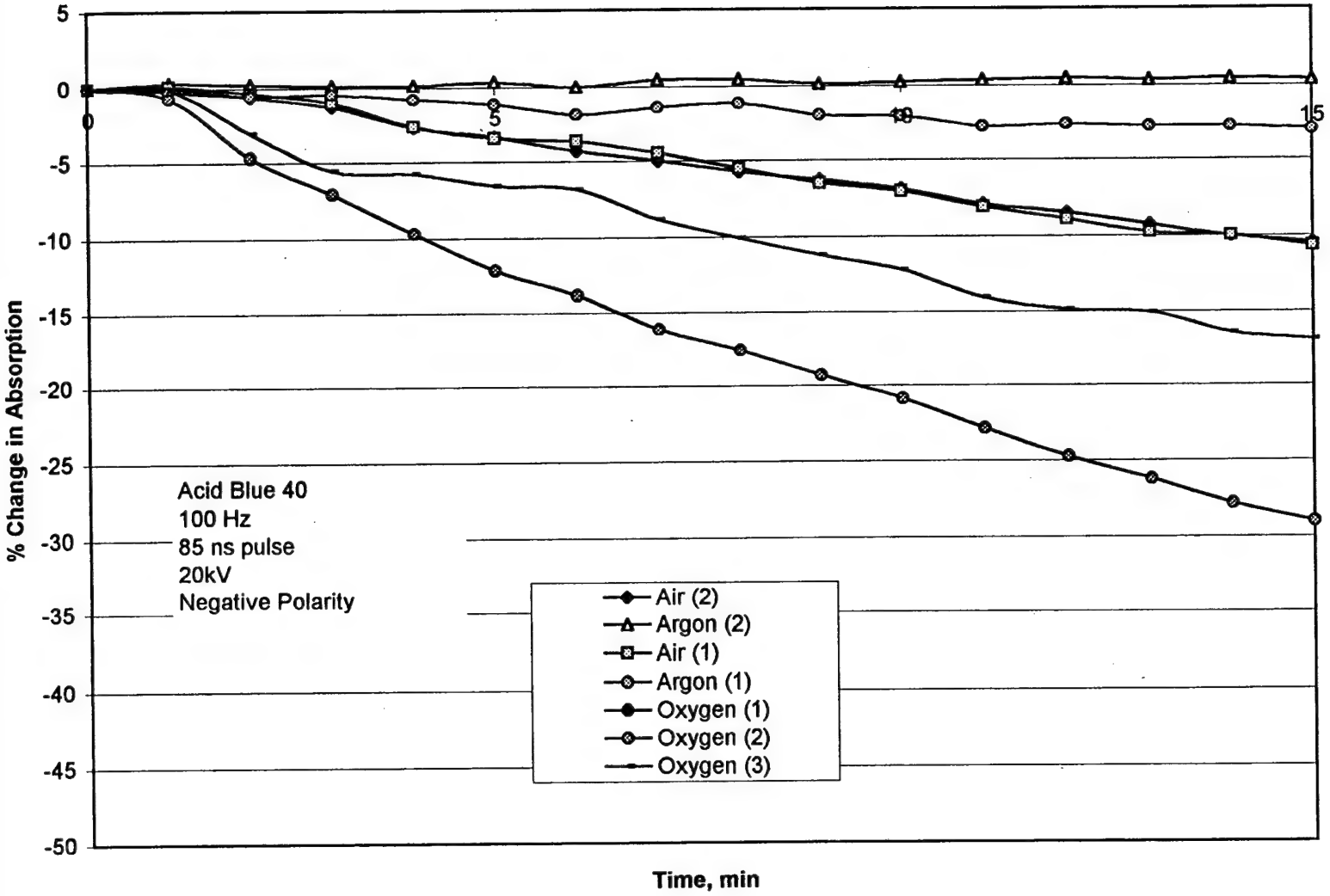

Figure 23 Gas Composition Sensitivity

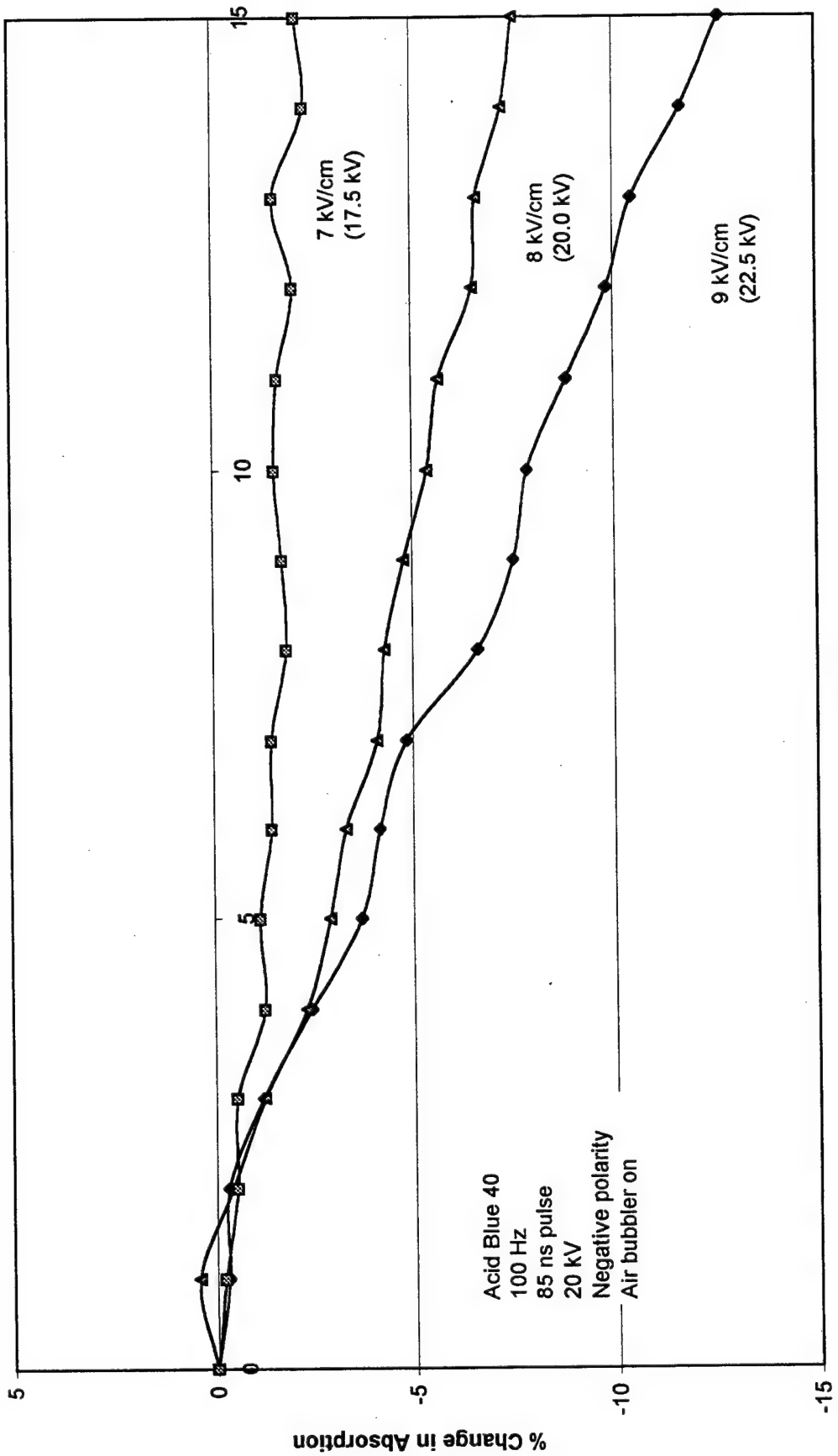

Figure 24 Field Strength Sensitivity

Excel/plasma/bludat24

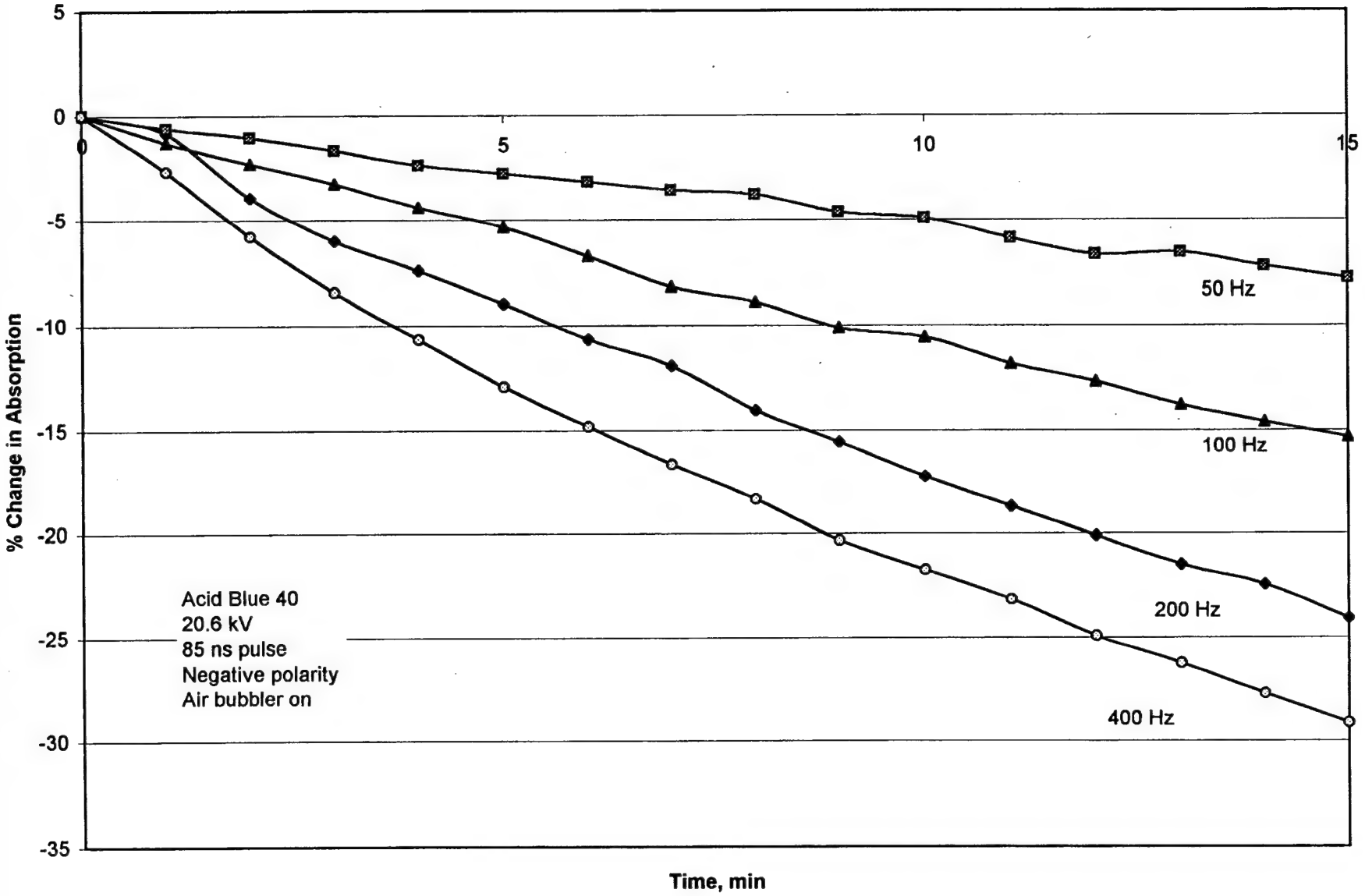

Figure 25 Electrical Pulse Rate Sensitivity

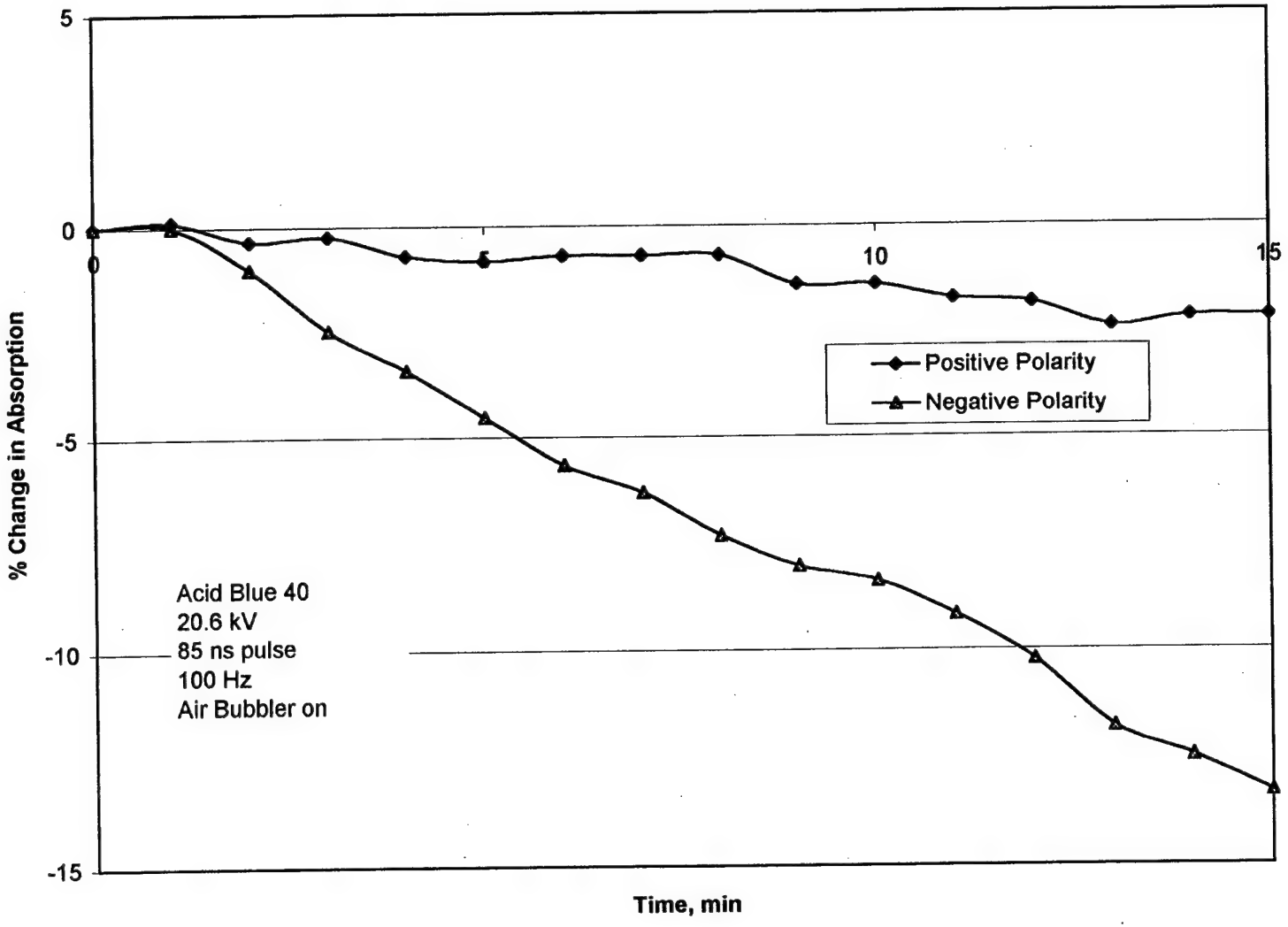

Figure 26 Electrical Polarity Sensitivity

Case 9. Conductivity. Figure 27 shows the effect of changing the conductivity of the solution. This study was conducted to determine how well the pulsed corona discharge would work with a sea water solution. The data show that addition of as little as 1 % sodium chloride stops the effect of pulsed corona discharges. It was observed that as salt content was increased, the electrical resistance of the reactor decreased. This resulted in a lower peak voltage developed across the reactor. For example, a peak voltage of only 8 kV could be developed across the reactor when the salt content was 2%. As the resistance of the fluid in the reactor decreases, the current flow through the reactor increases dramatically. Therefore, the electrical power going into the reactor increases, even though the peak voltage drops. The power consumed by the reactor increased by a factor of 4 when the salt concentration increased from 0% to 2 %. This increased power does not result in increased dye destruction. Rather, the power is consumed in moving salt ions and heating the water.

Case 10. Acidity. The pH of acid blue 40 solution was adjusted to pH 4 by addition of potassium hydrogen phthalate, and to a pH of approximately 11 by addition of sodium hydroxide. The results of corona discharge tests using these dye solutions are presented in Figure 28. The data indicate that acidic and basic solutions reduce the effectiveness of the plasma discharge process. This could be caused by electrical power being consumed by movement of the ions.

Case 11. Catalysts and Co-Reactants. Reference (2) reports that one of the major mechanisms of oxidation in the pulsed corona discharge process is production of hydroxyl radical from hydrogen peroxide by Fenton's reaction. Therefore, ferrous iron (in the form of iron(II) sulfate heptahydrate) was added to the dye solution. The solution was 1×10^{-4} M of acid blue 40 and 1×10^{-4} M of iron (II) in de-ionized water. The sulfate ion reduces the pH of the solution to about pH = 5. Figure 29 shows the test results. The addition of ferrous sulfate reduced the rate of decomposition of acid blue 40. This result indicates that hydrogen peroxide is not produced by the plasma discharges, and consequently, hydroxyl radicals are not formed by Fenton's reaction.

The addition of a small amount of powdered titanium dioxide to acid blue 40 solution appears to increase the reaction rate. The increase in reaction rate may be due to the catalyzing effect of TiO_2 in the presence of ultraviolet light emitted by the electrical discharges. Titanium dioxide is not soluble; the small particles remain in suspension and are circulated through the test apparatus along with the fluid.

Phenol Oxidation Studies. The goal of the second phase of this study was to reproduce the results on the oxidation of phenol reported in Reference (2). The method used to determine the effects of pulsed plasma discharges on phenol was ultra violet (UV) spectroscopy. A Perkin Elmer Lambda 9 UV-Visible-IR spectrophotometer was used to analyze the phenol samples.

Case 11. Baseline Analyses. Several experiments were performed to determine the UV absorption signatures of the products of reaction of phenol, hydrogen peroxide, and ferrous iron. The absorption spectra for phenol concentrations of 100, 75, 50, 25, and

12.5 ppm are presented in Figure 30. The peak absorption varies almost linearly with phenol concentration.

The absorption spectra for hydrogen peroxide concentrations of 2000, 1500, 1000, and 500 ppm are presented in Figure 31.

A 2000 ppm solution of hydrogen peroxide was mixed with a 100 ppm solution of phenol. The result is presented in Figure 32. Hydrogen peroxide by itself does not appear to be capable of significantly degrading phenol.

Experiments were conducted to determine the extent of degradation of phenol by Fenton's reaction. The results are presented in Figure 33. Figure 33 shows that when equal concentrations of hydrogen peroxide solution and phenol – ferrous iron solution are mixed, the concentration of phenol (as measured by peak absorption) is reduced by about 25 percent. Adding larger concentrations of hydrogen peroxide can reduce phenol concentration by as much as 50 percent. It is not possible to determine from these data the products of decomposition of phenol.

Case 12. Phenol Solution with Electrical Discharges. Figure 34 presents the experimental results after processing a 50 ppm solution of phenol in the plasma discharge reactor for a period of 15 minutes. Data are presented for three cases: pulses with air flow through the electrode, pulses with oxygen flow through the electrode, and air flow through the electrode only. The data indicate minimal (if any) degradation of phenol.

Case 13. Phenol Solution with Ferrous Iron and Electrical Discharges. Figure 35 shows the results when ferrous iron is added to the phenol solution. As before, no appreciable degradation of the phenol was observed.

Case 14. Phenol Solution with Titanium Dioxide and Electrical Discharges. Figure 36 shows the absorption spectrum for a 50 ppm phenol before and after processing. A small amount of TiO_2 was added to the phenol solution. The data indicate that a slight degradation of phenol may have taken place.

It was apparent from these tests that the author could not duplicate the results published in reference (2). Several suggestions were made to improve the performance of the experimental apparatus (reference 8). The most significant difference between the Navy pulse plasma experiments and the experiments conducted by Florida State University was the duration of the pulse. Reference (2) states that the FSU investigators used pulses of 500 to 1000 ns. The pulsed power supply supplied by Integrated Applied Physics, Inc., cannot generate pulses of 1 microsecond duration without modification to the unit. The power supply was modified to produce pulses of 1 microsecond duration and greater energy content, but the thyratron switch could not reliably handle the resulting increased current flow.

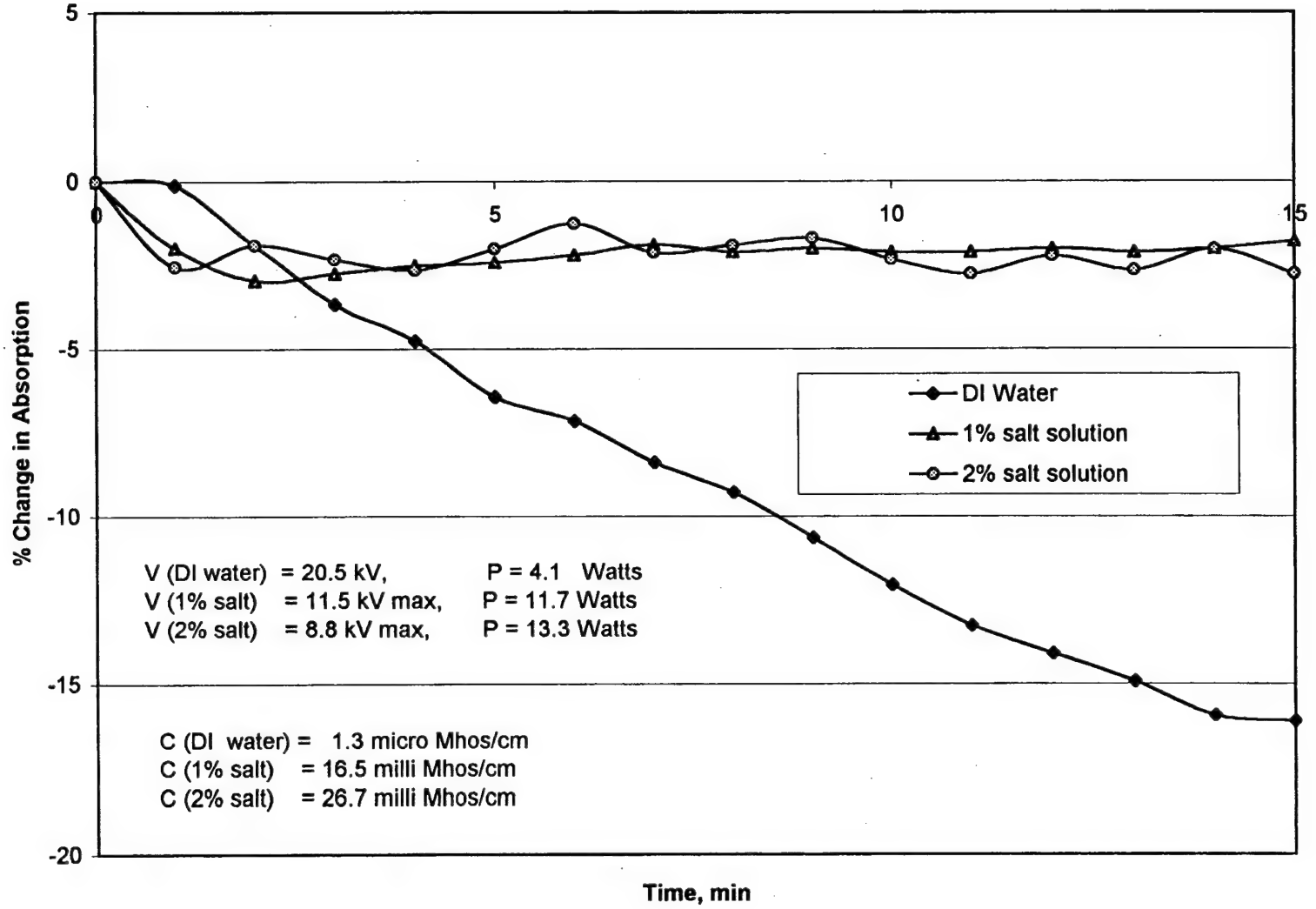

Figure 27 Solution Conductivity Sensitivity

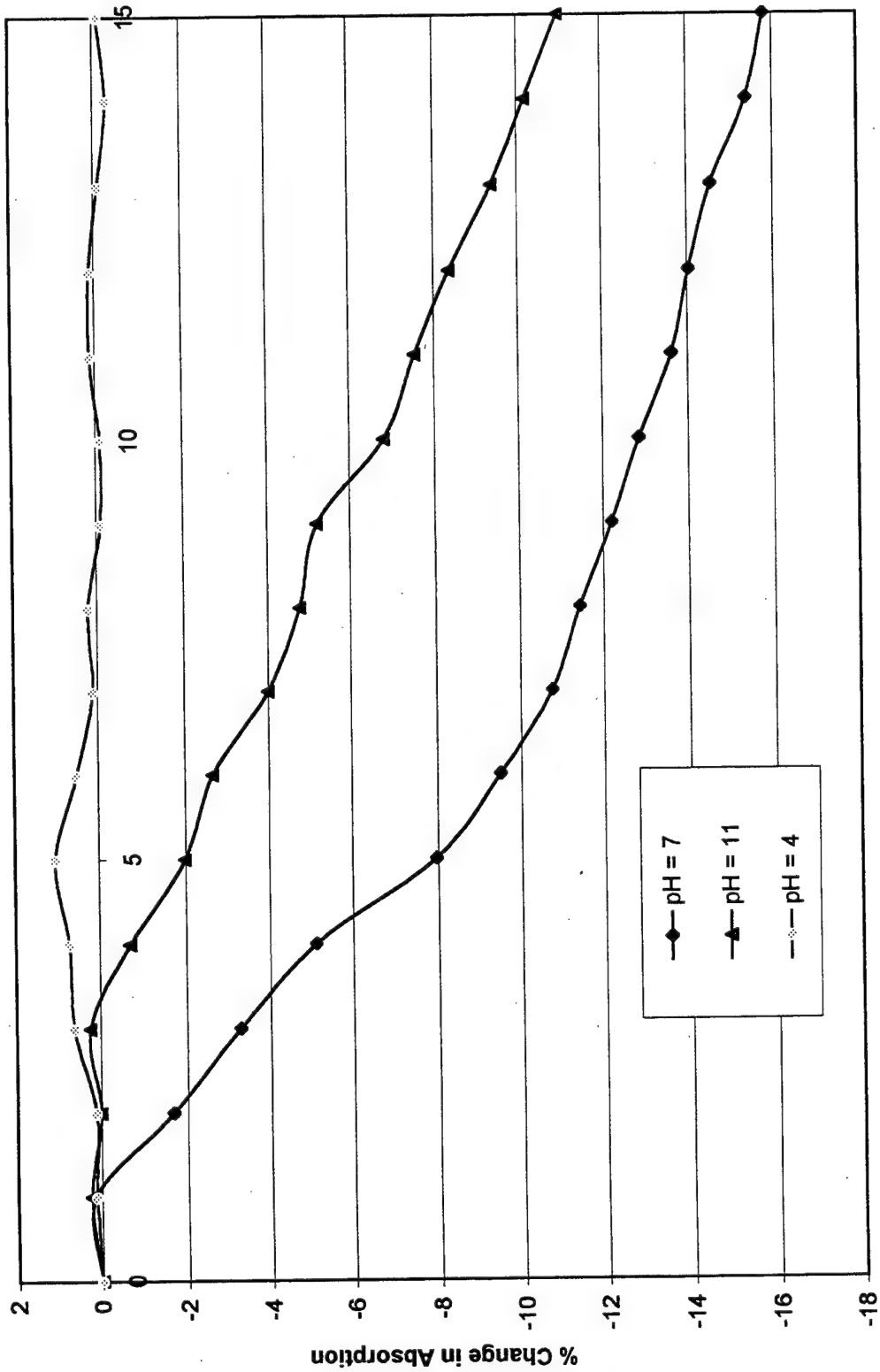

Figure 28 Solution pH Sensitivity

Excel/plasma/bludat55

Excel/plasma/fig29

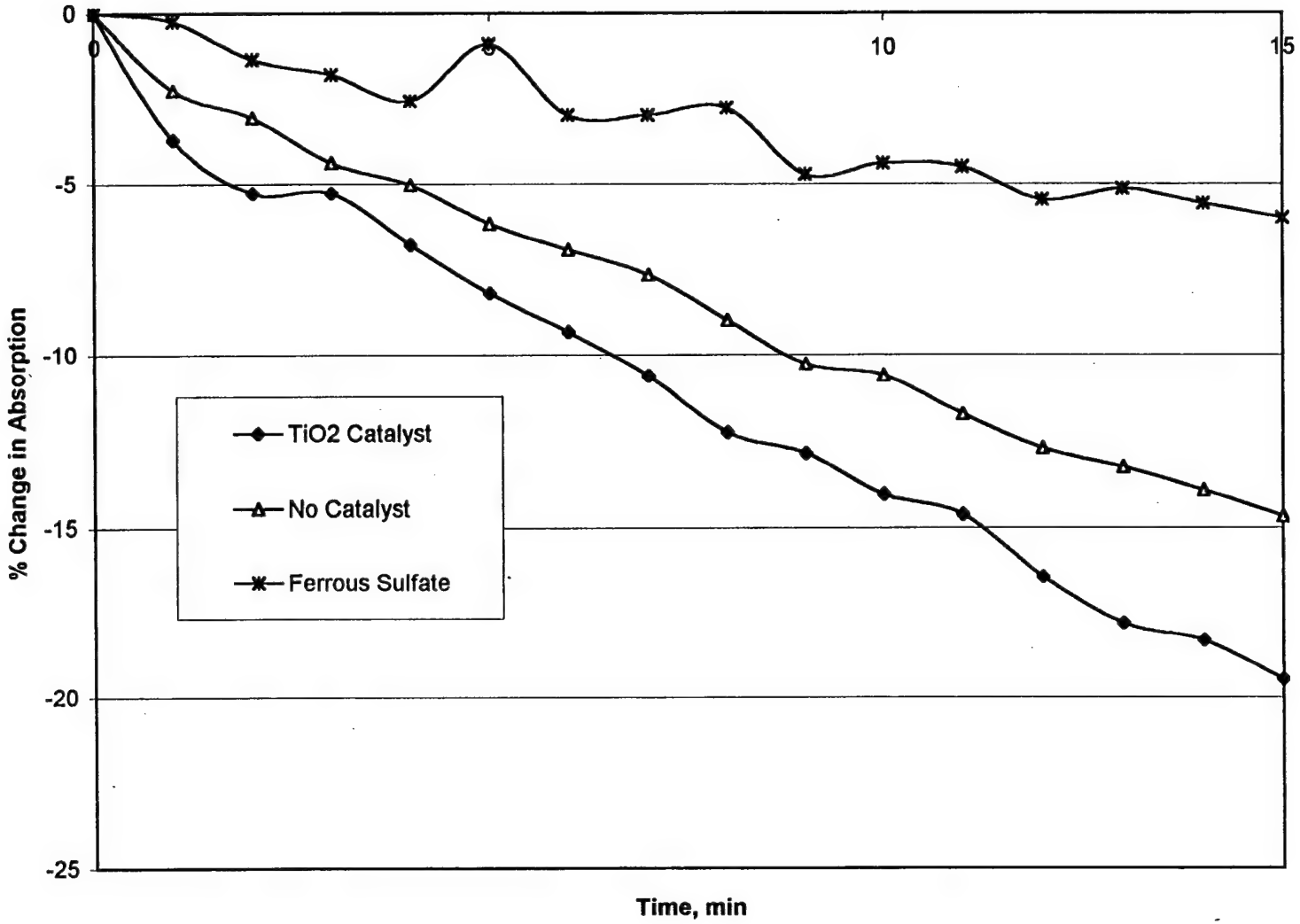

Figure 29 Catalyst and Co-reactant Sensitivity

Excel/plasma/fig30

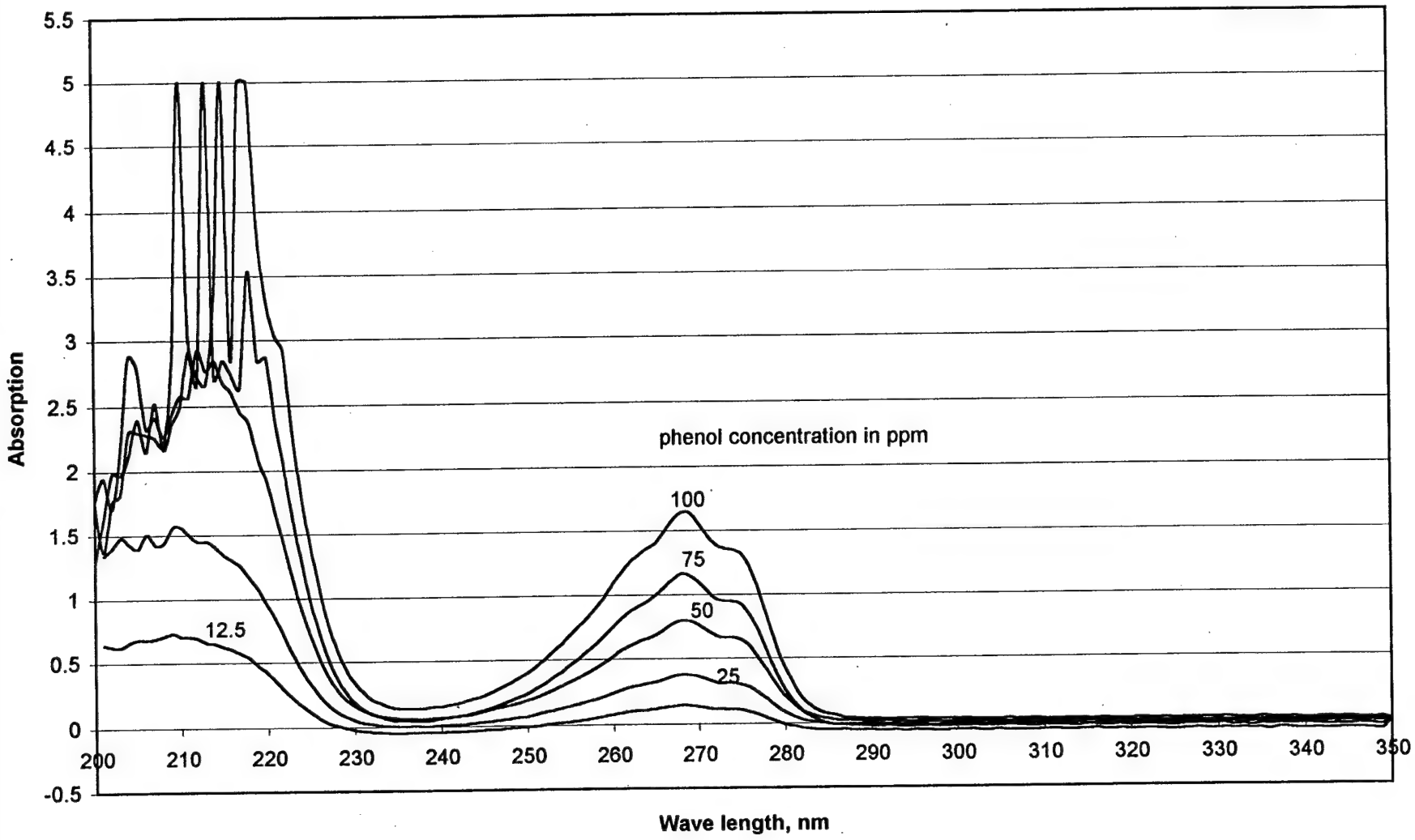

Figure 30 Absorption Spectra for Several Concentrations of Phenol in Water

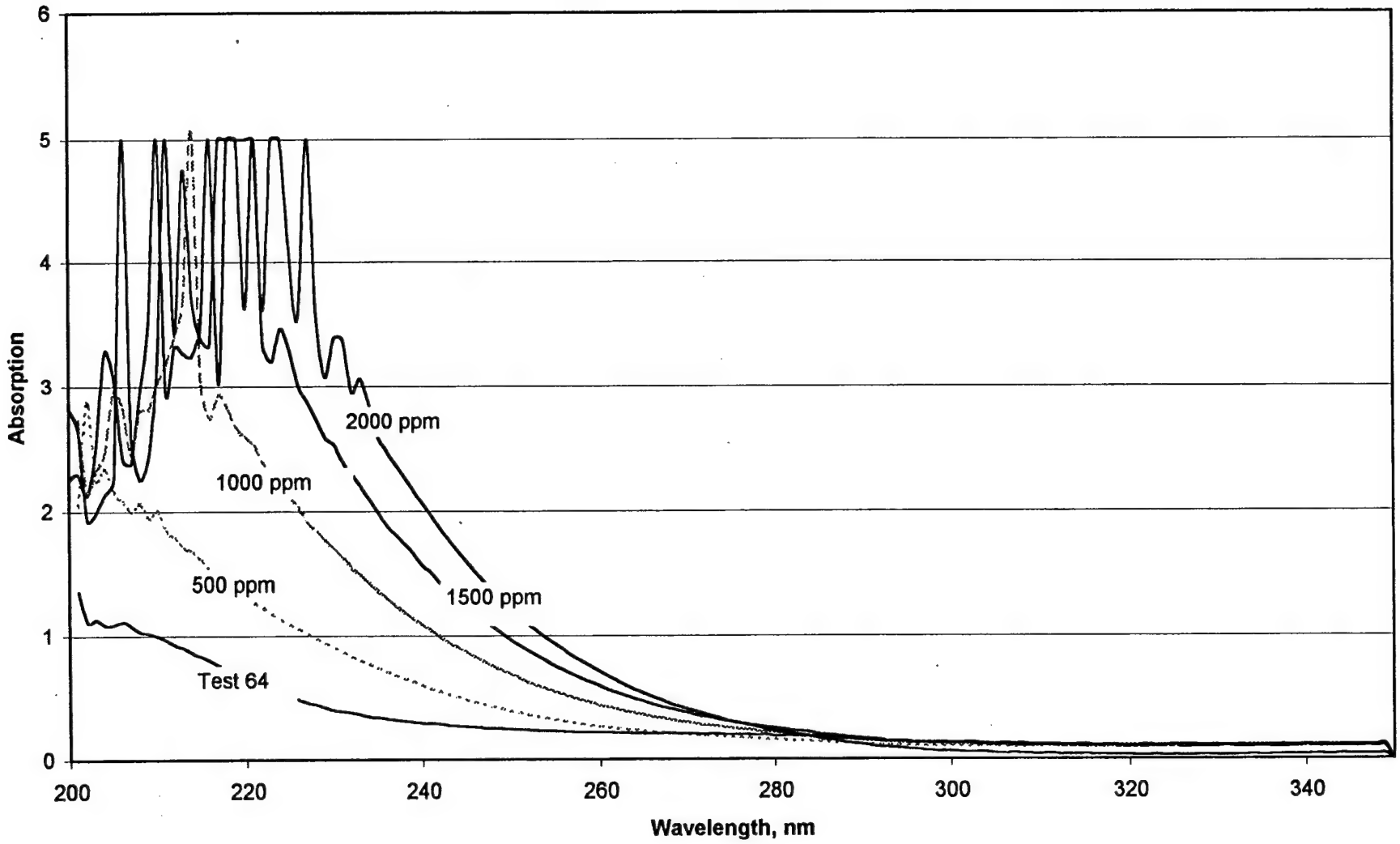

Figure 31 Absorption Spectra for Several Concentrations of Hydrogen Peroxide in Water

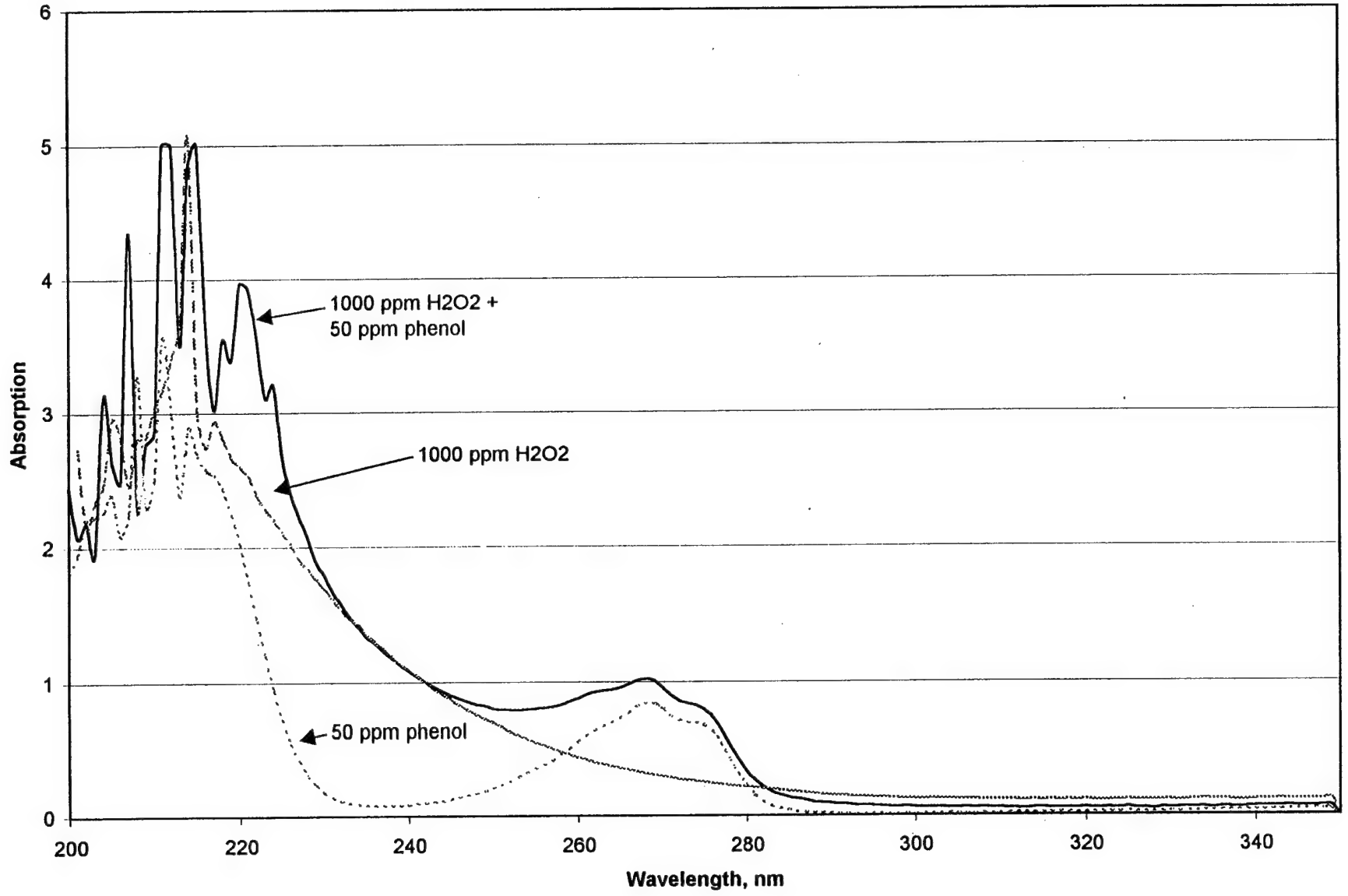

Figure 32 Absorption Spectra for a Mixture of Phenol and Hydrogen Peroxide

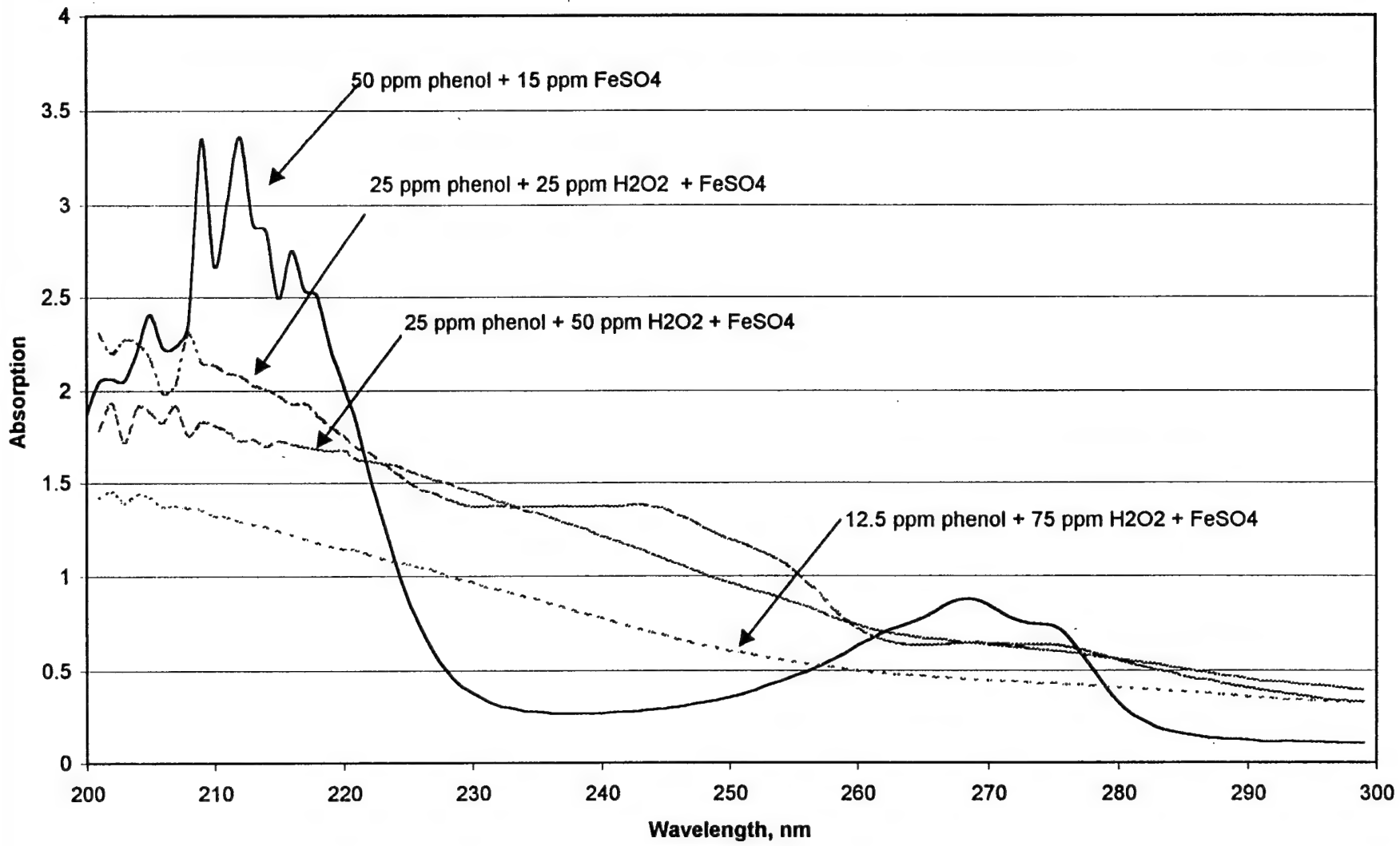

Figure 33 Results of Experiements with Fenton's Reaction

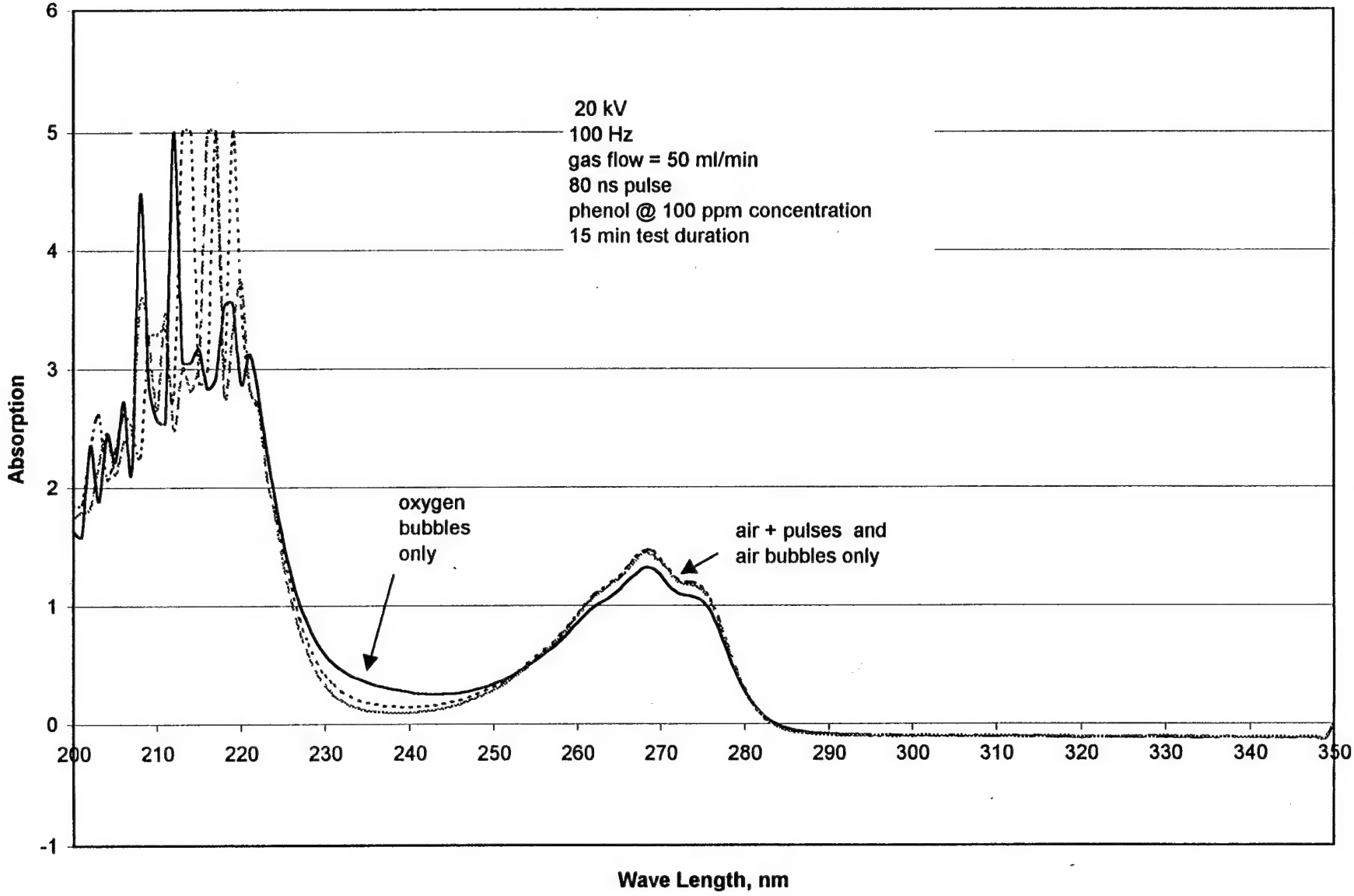

Figure 34 Spectra for Plasma Discharges in Phenol Solution

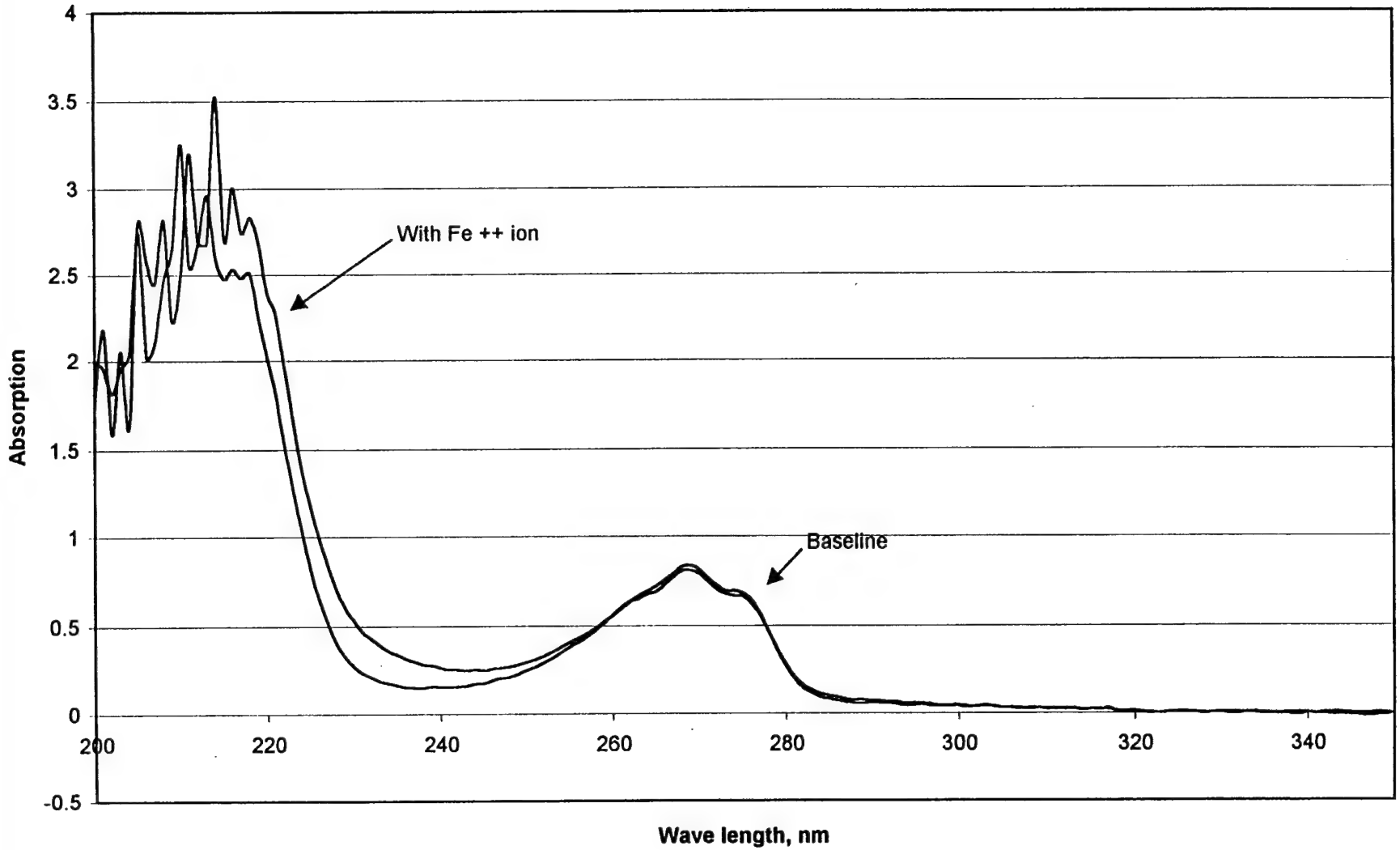

Figure 35 Spectra for Plasma Discharges in Phenol Solution Containing Ferrous Ion

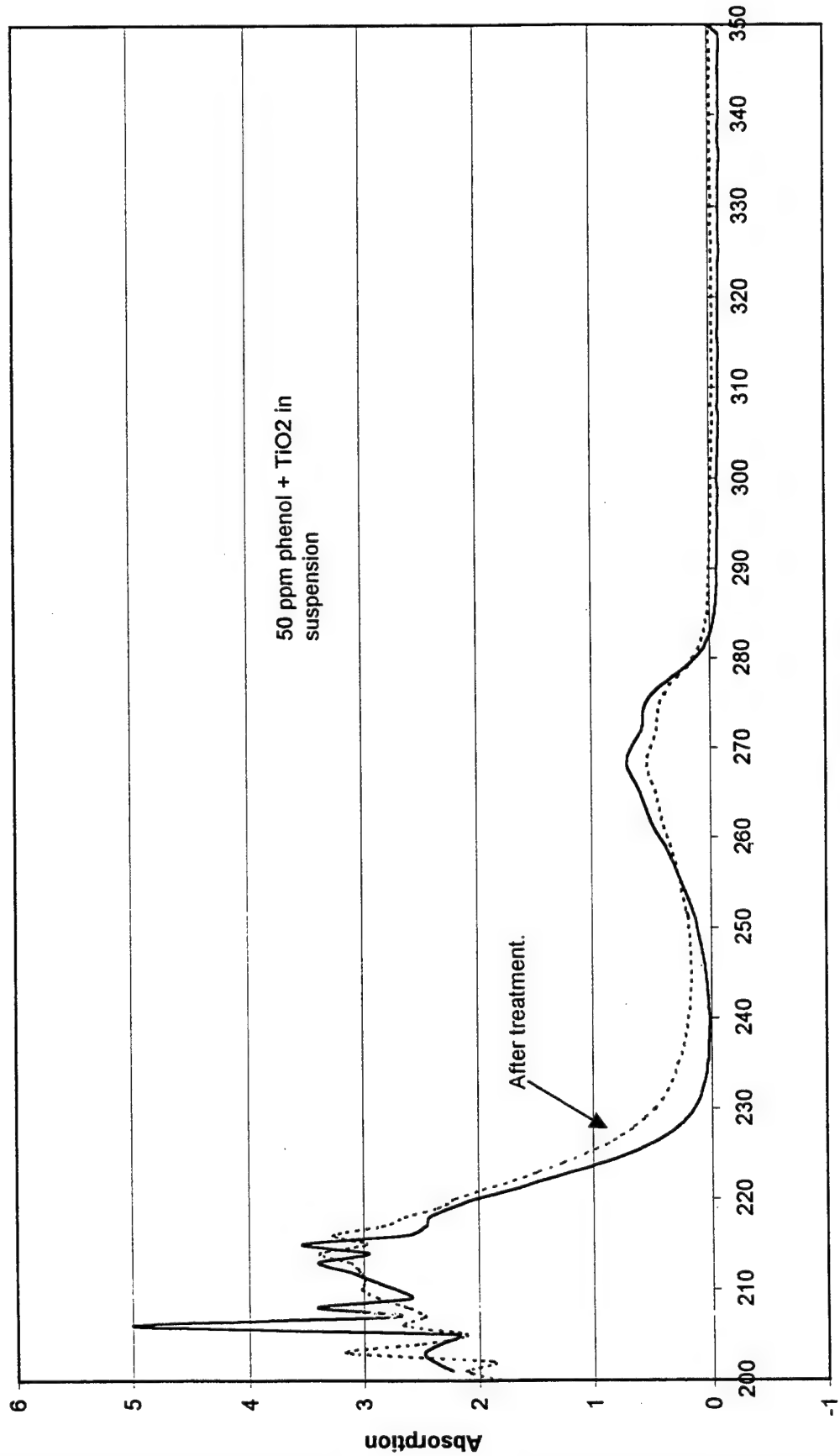

Figure 36 Spectra for Plasma Discharges in Phenol Solution Containing Titanium Dioxide

Excel/plasma/test37

To overcome this inherent design limitation with the Integrated Applied Physics, Inc. power supply, a new power supply was assembled. The power supply was designed with the aid of *Electronics Workbench* software from Interactive Image Technologies, Ltd. The circuit diagram of the power supply is presented in Figure 37. The core of the design is variable voltage, variable current power supply made by Glassman High Voltage, Inc. The Glassman power supply (model LX60R33) can provide 0-60 kV DC at 0 to 33 mA. The power supply charges special, high energy, storage capacitors through a resistor. When the voltage across the capacitors reaches the breakdown voltage of the spark gap, the capacitors discharge across the gap. The spark gap breakdown voltage is determined by the spacing of the electrodes in the spark gap and the composition, temperature, and pressure of the gas contained in the spark gap enclosure. For air at standard temperature and pressure, the breakdown voltage is 30 kV/cm. The duration of the discharge pulse is determined by the discharge time constant (the product of the capacitance and the load resistance), the ratio of the load resistance to the charging resistance, and the characteristics of the spark gap. The pulse frequency was observed to vary between 10 and 50 Hz. The pulse frequency was observed to increase with decreasing load resistance. A consistent pulse frequency could be obtained by replacing the static spark gap with a motor driven spark gap switch.

The power supply is designed to produce up to 5.5 J/pulse. This is approximately 10 times more energy per pulse than was delivered by the original power supply. Typical operating conditions are 1 to 1.5 J/pulse. Recent work at Florida State University (Reference 9) suggests that 0.8 to 1.3 J/pulse is required to degrade phenol.

Typical current and voltage waveforms for pulsed corona discharges in de-ionized water are presented in Figures 38 and 39. In this particular example, the energy stored in the capacitors is 1.03 J. As Figure 38 shows, most of the energy discharge occurs over the first microsecond. During this time, highly conductive channels (or streamers) are formed in the water. A significant current flow (over 70 A in this case) then ensues. The energy discharged during this initial stroke was measured to be 0.25 J. The conductive channel then collapses and is replaced by a conductive path with much higher electrical resistance. The remaining energy in the pulse (0.78 J in this example) is then dissipated at a much slower rate. In this case, the remainder of the pulse is dissipated at a low current (about 100 mA) over a period of about 6 milliseconds (a period 6000 times longer than the initial stroke).

Case 15. Phenol Solution with Electrical Discharges. Case 13 was repeated using the more powerful pulser. The initial applied potential was 35 kV, but this produced almost continuous spark-over. The applied voltage was lowered by 2.5 kV increments to 27.5 kV, where spark-over was only intermittent. Pulse frequency varied between 10 and 30 Hz. The Pulse duration was approximately 1 millisecond. Current flow was approximately 10 to 20 Amperes per pulse. The relatively long pulse duration is due to the low conductivity of the solution. The results are presented in Figure 40. After 15 minutes of operation, no decrease in the concentration of phenol was achieved.

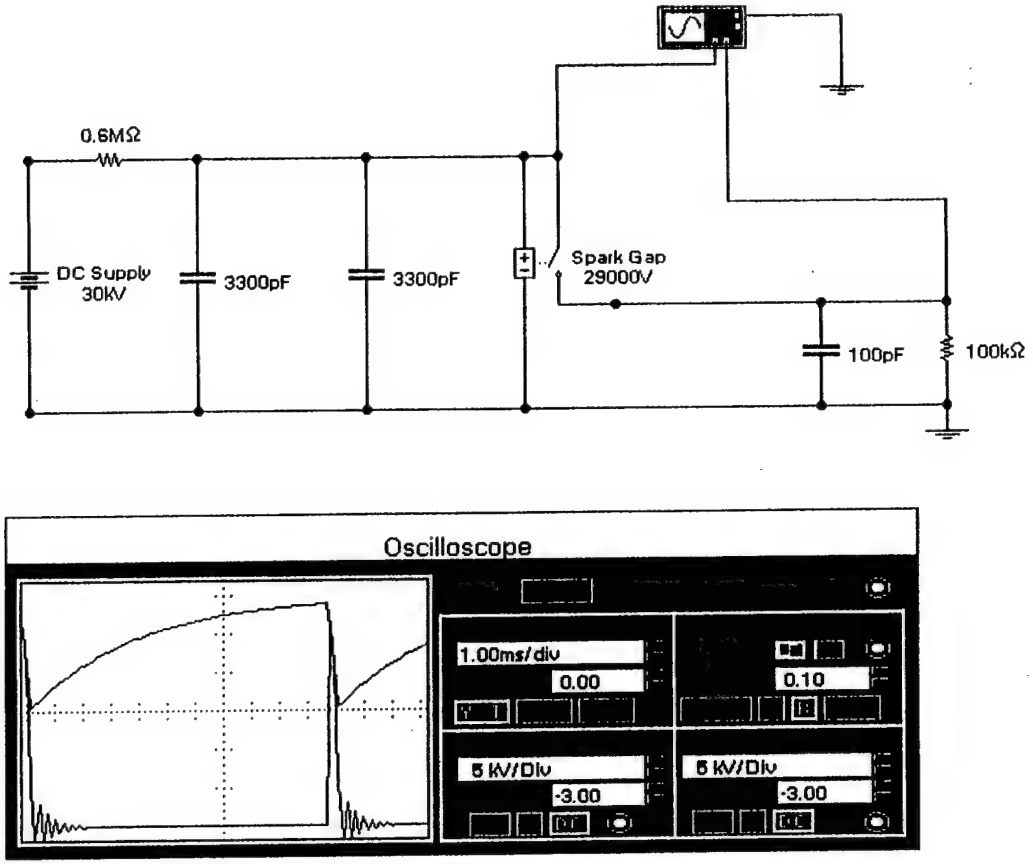

Figure 37 Circuit Diagram of NFESC Pulse Power Supply Design

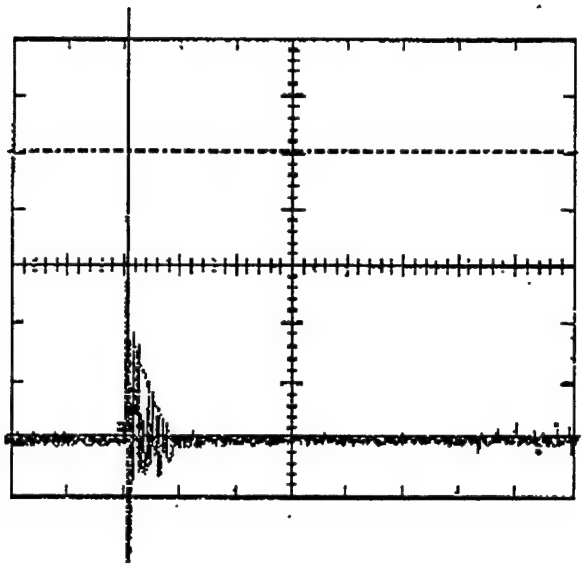

X axis: 1 unit = 1 microsecond Y axis: 1 unit = 10 Amperes

Figure 38 Current Flow in De-ionized Water

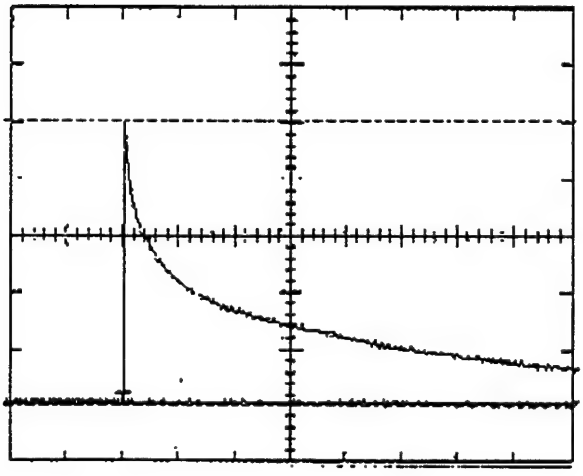

X axis: 1 unit = 500 microseconds Y axis: 1 unit = 5000 Volts

Figure 39 Voltage Discharge in De-ionized Water

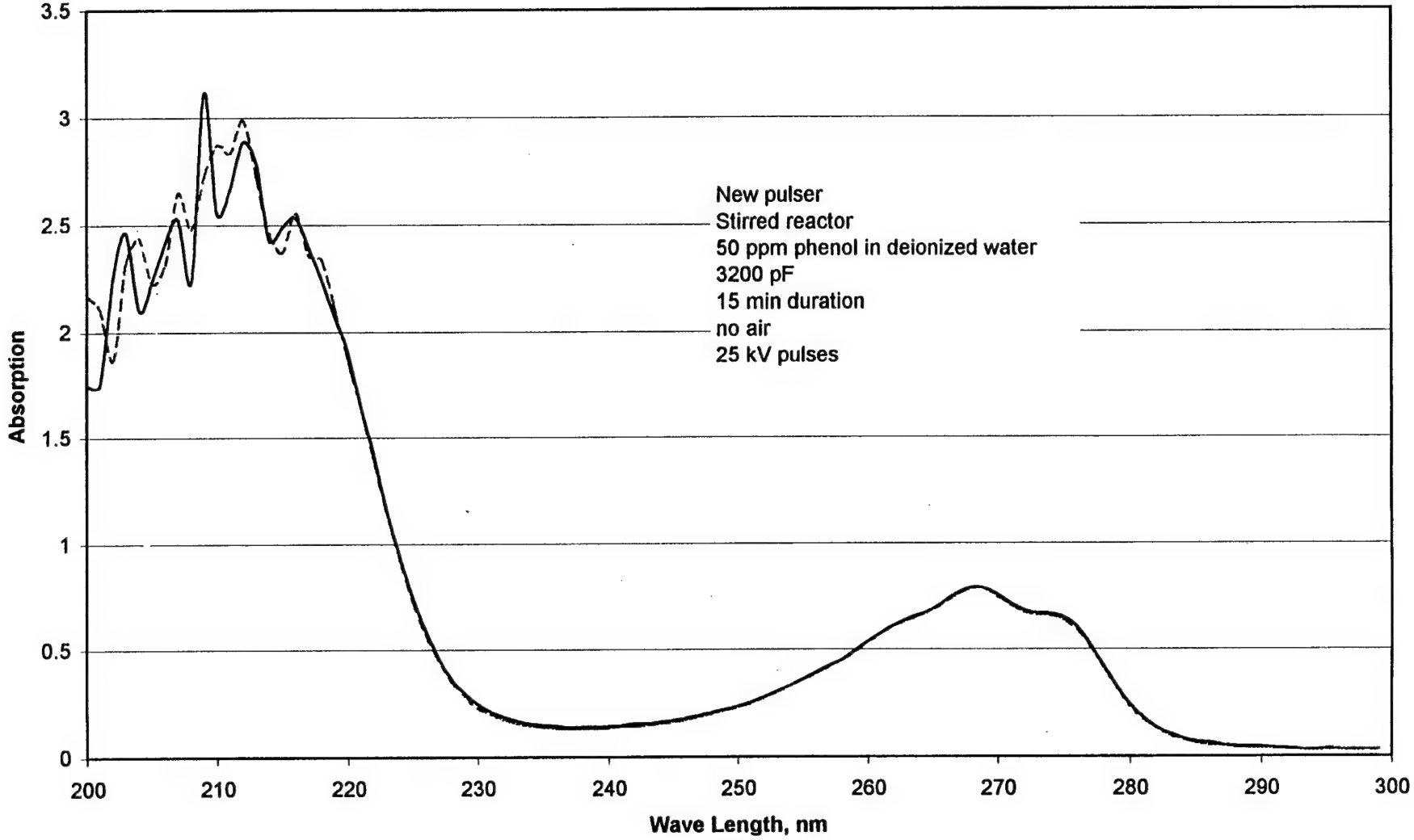

Figure 40 Degradation of Phenol Using High Power Pulser (no Fe++)

Case 16. Phenol Solution with Ferrous Iron and Electrical Discharges. Case 14 was also repeated using the new pulser. Ferrous iron heptahydrate was added to the phenol solution in the amount recommended in Reference 9. The measured conductivity of the solution was 52 x 10^{-6} Mhos/cm. Pulse duration was approximately 20 microseconds. Typical current values were 90 to 100 Amperes per pulse. The higher current flow (as compared to Case 16) is attributed to the higher solution conductivity. Corona discharges were also less regular than those observed for Case 16. The results are presented in Figure 41. No change in the initial concentration of phenol was observed.

Flow-Through Reactor Studies. The electrical resistance of the reactor vessel has a significant effect on the ability to generate streaming coronas. Coronas are easily produced in a reactor vessel with a high electrical resistance, such as one filled with de-ionized water. However, when de-ionized water is replaced with ordinary tap water, corona discharges are often weak and intermittent. The conductivity of tap water is so high that a high electrical stress field cannot be developed, and the electrical current is simply conducted through the water.

The electrical resistance of a reactor vessel is approximately described by the relationship:

$$R = d/(k*A) \qquad (7)$$

where

R = electrical resistance, Ohms

d = distance between electrodes, cm

A = characteristic area of electrodes, cm^2 and

k = electrical conductivity of the solution, Mhos/cm.

Therefore, for a given value of solution conductivity, the electrical resistance of the test vessel can be increased by increasing the distance separating the electrodes and reducing the electrode area.

A new, smaller volume, high resistance test cell was designed and built (Figure 42). The cell is a flow through design and consists of a clear Lexan tube 2.5 cm in diameter with a needle electrode and the bottom of the tube and perforated copper disk electrode at the top of the tube. The distance between the two electrodes is 5 cm. Water is circulated through the reactor by a small pump.

Table 4 compares the geometry and electrical characteristics of the stirred reactor vessel and the flow through reactor vessels. Measured electrical resistance is presented for two cases: de-ionized water (k = 1.3 x 10^{-6} Mhos/cm) and tap water (k = 143 x 10^{-6} Mhos/cm).

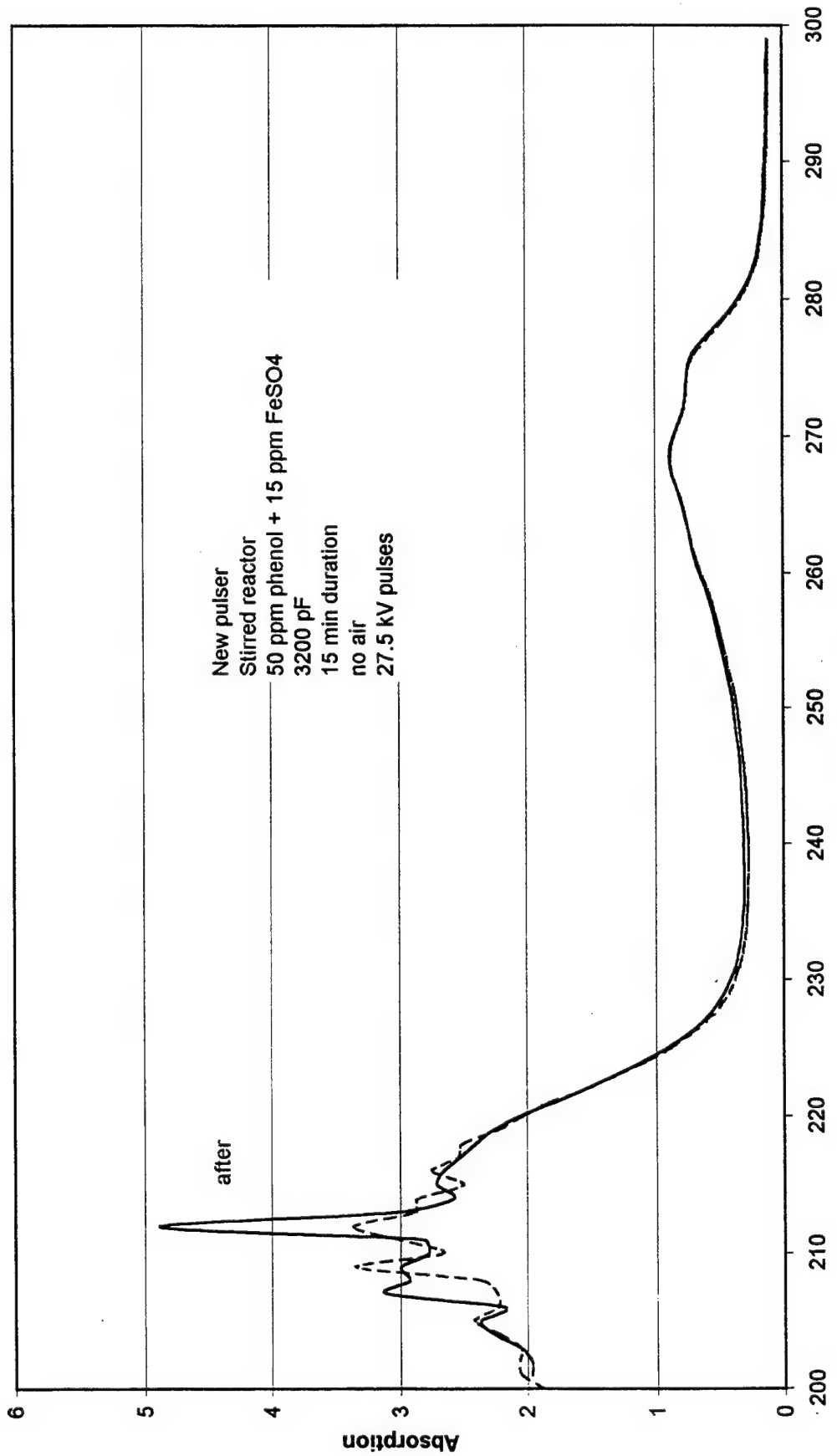

Figure 41 Degradation of Phenol Using High Power Pulser (with Fe++)

Excel/plasma/test82

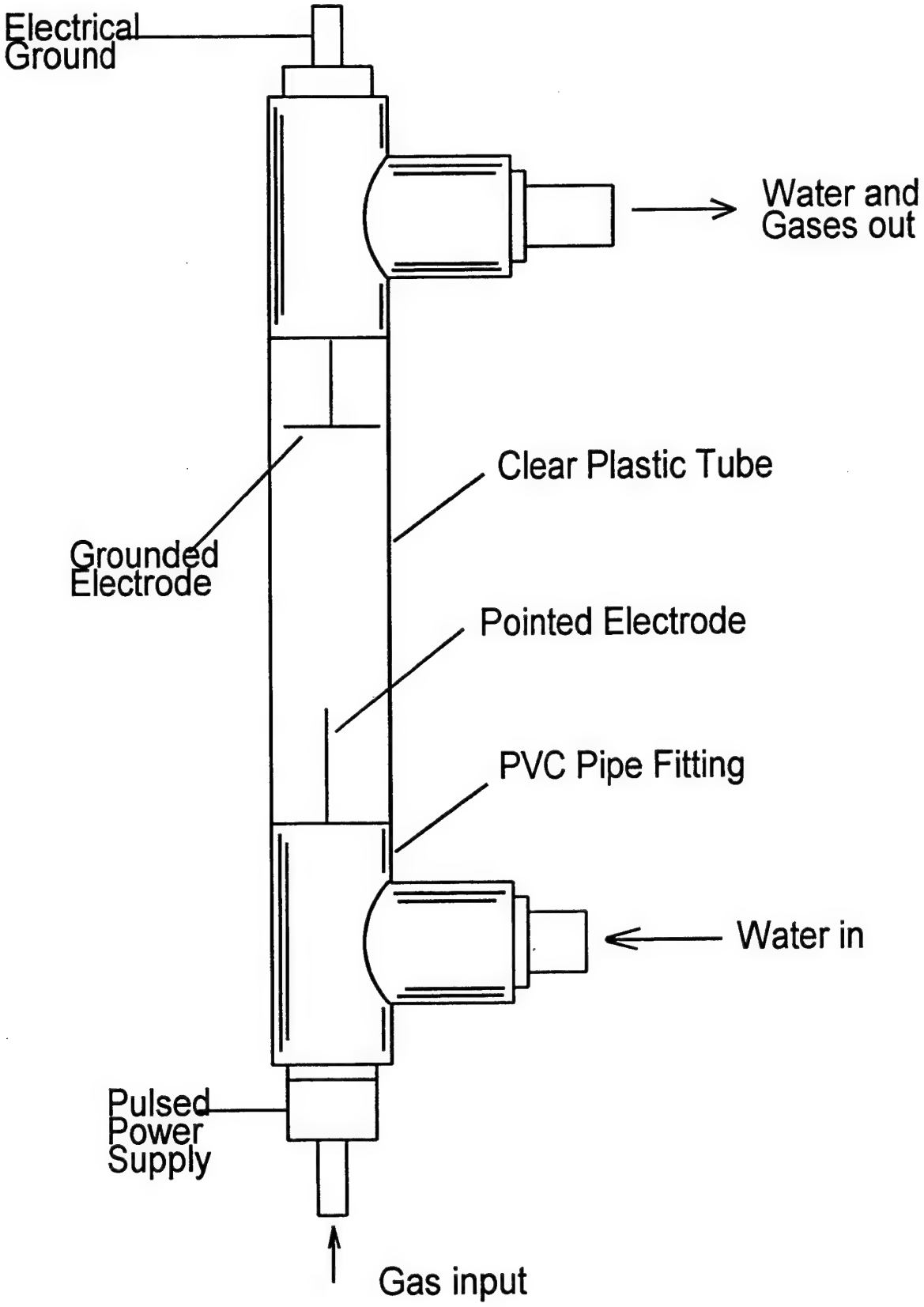

Figure 42 Drawing of Flow-through Reactor

Table 4 Comparison of Electrical Characteristics of Two Reactor Vessels

Reactor	Area, cm^2	R de-ionized water , Ohms	R tap water, Ohms
Large, stirred	150	160,000	250
Small, flow through	3	200,000	800

Cell resistance was measure with a capacitive discharge type impedance tester (Biddle Instruments, Inc., Blue Bell, PA). Solution conductivity was measured with a conductance meter (Yellow Springs Instruments, Yellow Springs, OH). A load resistance of 800 Ohms is an approximate match to the output impedance of the power supply, so energy transfer to the load should be efficient.

Current and voltage data for the small flow-through reactor are presented in Figures 43 and 44. The data are for tap water. As can be seen by comparison of Figures 43 and 44 with Figures 38 and 39, the pulse is short and the current and voltage waveforms are temporally consistent. The discharges produced under these conditions were bright white spots of light at the tip of the pointed electrode, with shorter and less numerous plasma streamers. In this experiment, the measured energy per pulse (the area under the curve of the product of voltage times current versus time) was 2.5 Joules. The calculated energy in the capacitor bank equals

$$E = 0.5^* C * V^2 = 0.5^*(3200 \times 10^{-12}) * (40{,}000)^2 = 2.56 \text{ J} \qquad (8)$$

Thus, about 100% of the stored energy was delivered in a short duration pulse.

The results presented above indicate that there is an optimum value of solution conductivity. If the value of conductivity is too high, no discharges are produced: the current simply flows from one electrode to the other. When the conductivity is too low, a high field stress is produced, but little current (and therefore little power) is input to the solution. At the optimum value of solution conductivity (or alternatively, optimum vessel geometry for a specified fluid conductivity), a large amount of energy can be input to the fluid in the form of brief pulses.

Case 17. Phenol Solution with Ferrous Iron and Electrical Discharges. Case 15 was repeated using the flow through reactor vessel in place of the stirred reactor vessel. The intent of this experiment was to raise the electrical resistance of the load. Since the phenol-ferrous iron solution is comparatively conductive, the only method available to increase the resistance is to change the geometry of the reactor vessel. The results are presented in Figures 45 and 46. The measured resistance of the reactor vessel was 33 k Ohms; too high a value for significant energy transfer to the solution. A small amount of sodium chloride was added to the solution to reduce the cell resistance to about 1 k Ohm. The result is presented in Figure 46. No degradation of phenol was detected in either of these experiments.

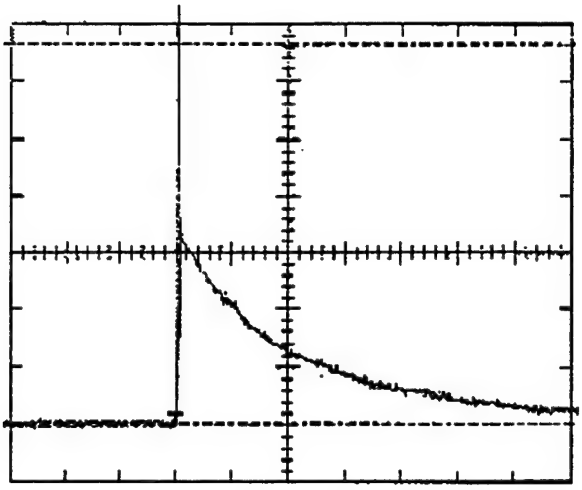

X Axis: 1 unit = 10 microseconds Y Axis: 1 unit = 20 Amperes

Figure 43 Current Flow in Tap Water

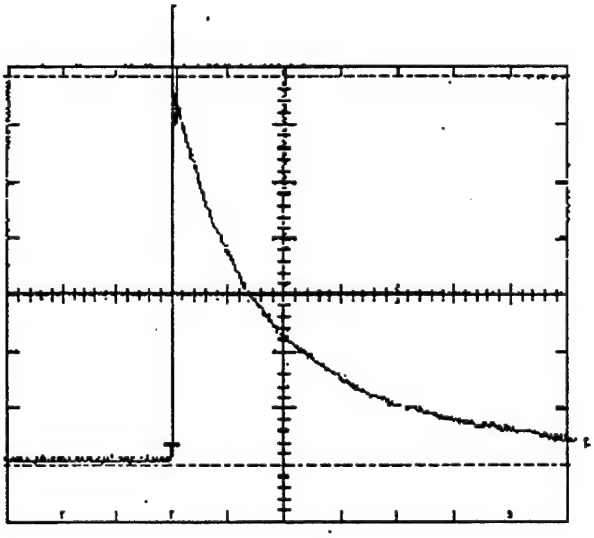

X Axis: 1 unit = 10 microseconds Y axis: 1 unit = 5000 Volts

Figure 44 Voltage Discharge in Tap Water

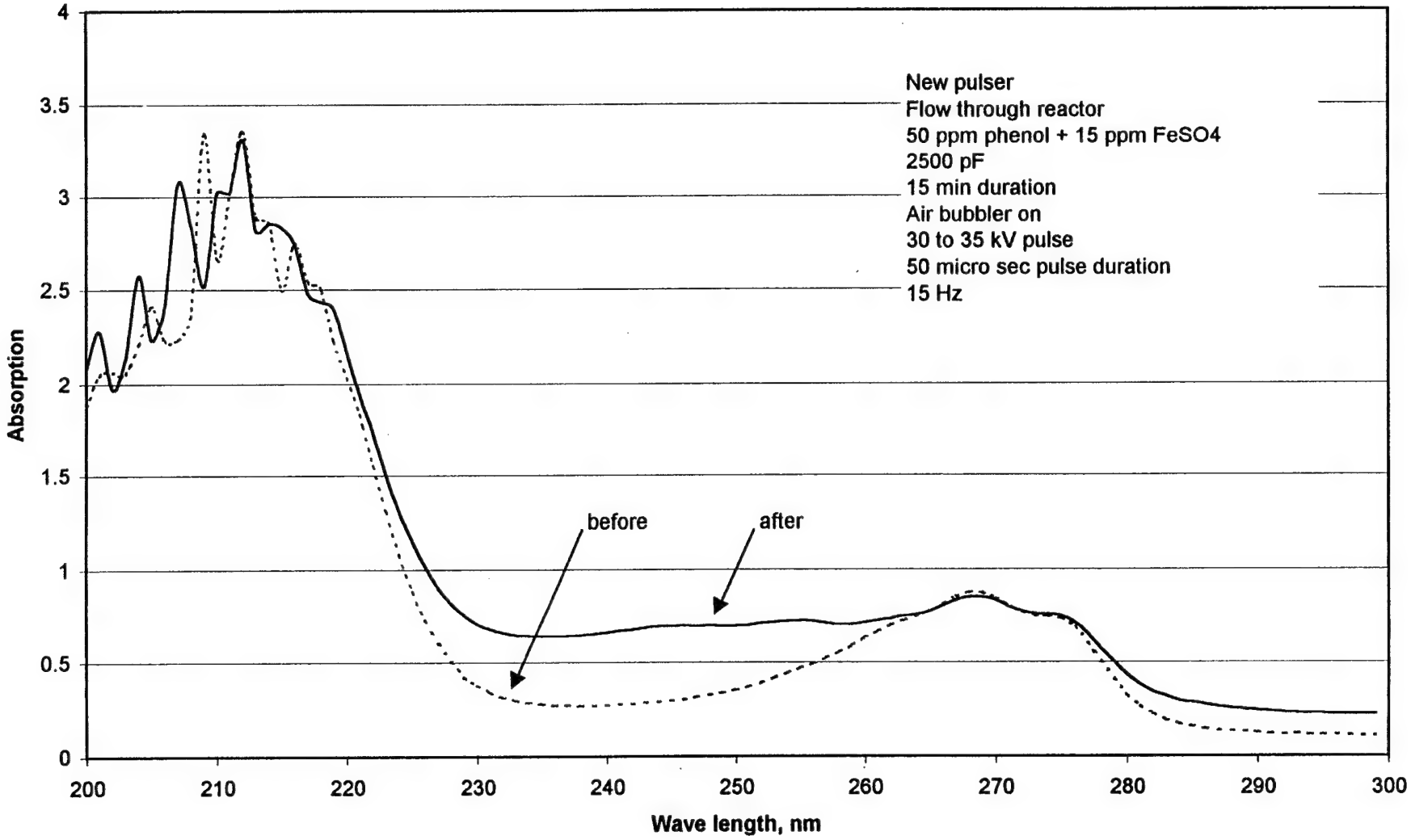

Figure 45 Degradation of Phenol in Flow-through Reactor (High Load Impedance)

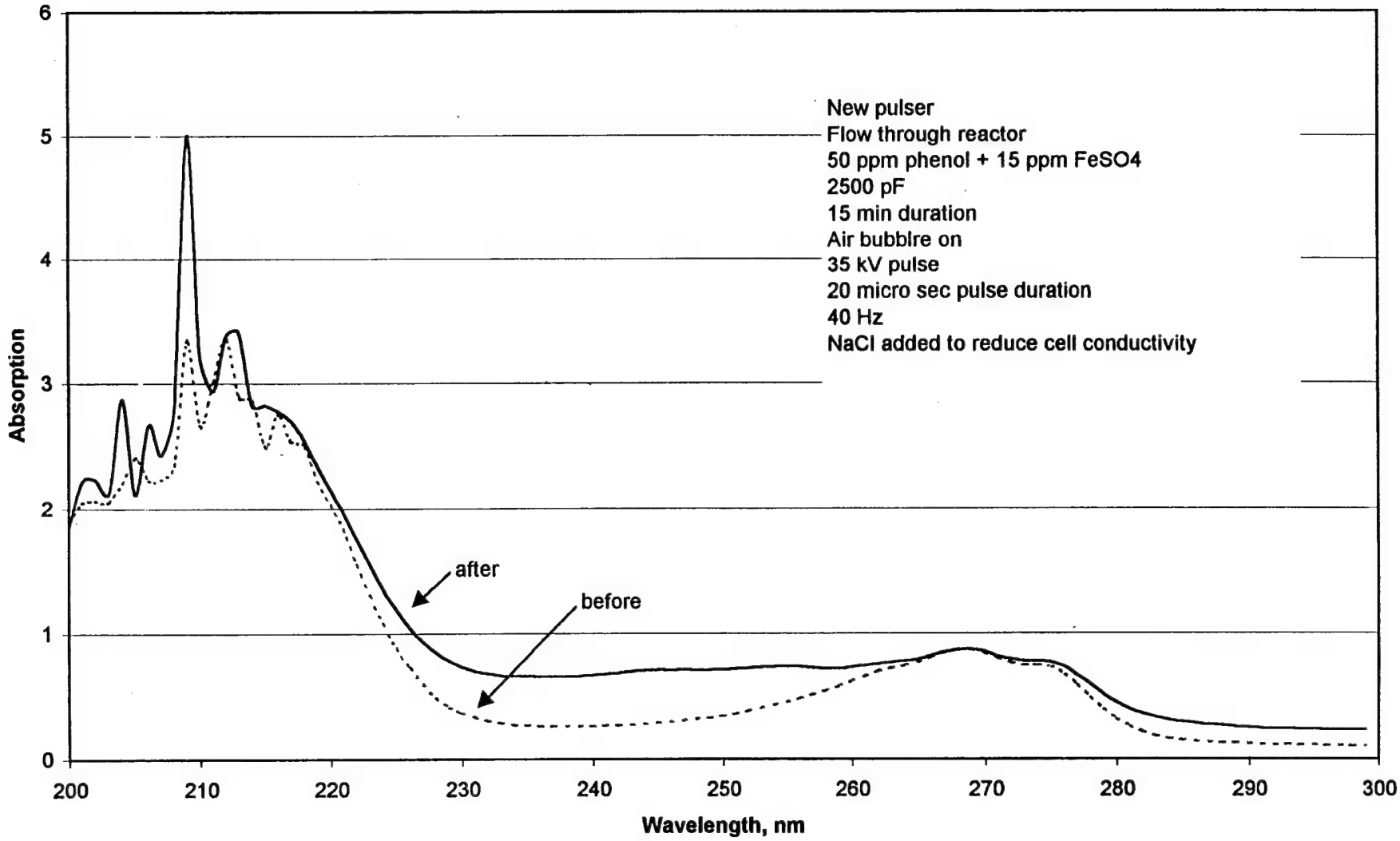

Figure 46 Degradation of Phenol in Flow-through Reactor (Low Load Impedance)

Results of Other Recent Investigations. Figure 47 (from reference 9) presents data on the byproducts of the degradation of phenol in a pulsed streaming corona discharge apparatus. These data are for 100 ppm phenol and 485 μM ferrous sulfate in a 1 L reactor vessel. These data show that after 15 minutes of operation, about 28 percent of the phenol is converted to other chemical species. Eighty four percent (by mass) of the products of the degradation of phenol are catechol, resorcinol, and hydroquinone. These compounds result from adding one more hydroxyl group to the phenol molecule. Catechol, resorcinol, and hydroquinone have the same formula weight and differ from each other only by the position of the –OH group on the benzene ring. Catechol is classified as a toxic corrosive. Resorcinol is classified as a toxic irritant. Hydroquinone is classified as a toxic cancer suspect agent. The remaining 16% of the carbon in phenol was assumed to be other oxidation products such as formic and oxalic acids. Note that although the applied voltage used for the experimental results presented in Figure 47 is about twice that used for the experiments results presented in Figure 6, the measured degradation of phenol is substantially less. Figure 6 shows 100 percent degradation; Figure 7 only 28 percent.

Process Development Issues. Even if it is assumed that the pulsed corona discharge process can be made to work as well as the results presented in Figure 6 show, experience with experimental apparatus indicates that formidable engineering challenges will need to be overcome for the process to be practical.

First, experience shows that streaming corona discharges are produced in an aqueous solution only when the solution has a very low value of electrical conductivity. Experience shows that corona discharges are difficult to produce in ordinary tap water. In a practical application it would probably be very difficult to maintain low solution conductivity. Even if the process started out with de-ionized water as the process solution, the accumulation of suspended particles, ions, and gases in the solution would quickly raise the conductivity to the point where corona production would cease. This effect has been observed in several experiments. Initially, a corona discharge is produced with each pulse output by the power supply. As the experiment progressed however, fewer corona discharges were produced and, finally, corona production ceased (even though the power supply continued to output pulses). It was observed that the duration of the pulses decreased with increasing time, indicating that the conductivity of the fluid was increasing.

The second engineering challenge is related to processing volume. The active processing volume is very small: a region of perhaps 1 cubic millimeter (at the tip of the discharge point). To make the process efficient it is required to configure a system that has a large number of discharge points in a small reactor volume. This is not easily done. Experiments were performed using the stirred batch reactor equipped with multiple discharge points. Both 5-point and 33-point configurations were investigated. The conclusion is that the presence of additional discharge points reduces the effective field strength. Fewer, weaker discharges were observed with the 5-point configuration. No discharges were observed with the 33-point configuration. These results confirm the predictions of computer models of multi-point discharge configurations. The computer model indicates that adding a second discharge point 2.5 cm from the first reduces the

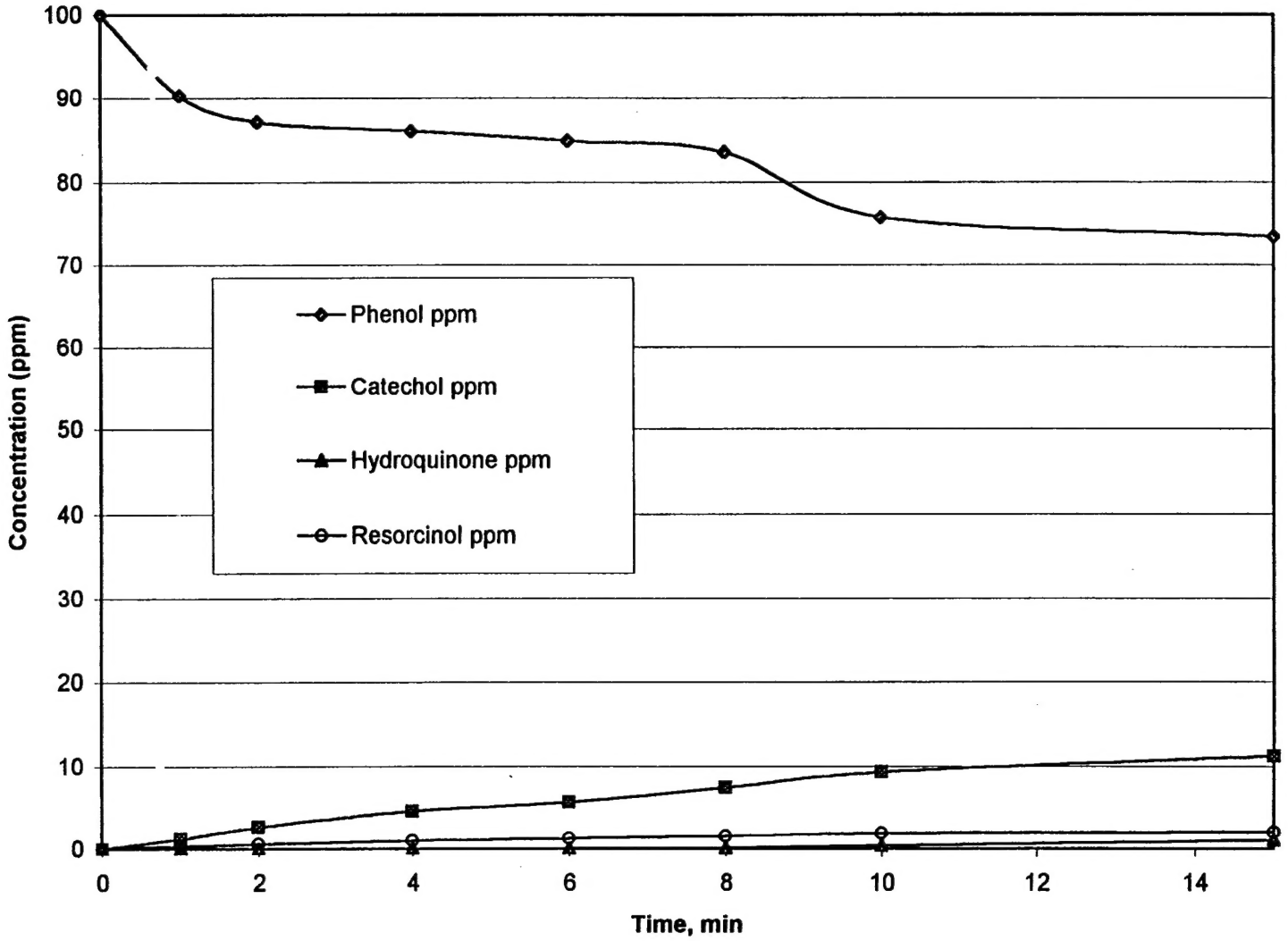

Figure 47 Degradation of Phenol by Pulsed Corona Discharges

field strength from about 130 kV/cm to about 50 kV/cm. Additional discharge points, or more closely spaced discharge points, further reduce the peak field strength. In the limit, an array of many discharge points produces the same electric field as two parallel plates. That is to say, in the limit the electrical field strength is reduced to the potential difference between the electrodes divided by the electrode separation distance.

The wire-in-tube configuration was also investigated. To test this configuration, the 1L stirred reactor vessel was equipped with a small diameter (2 mm) threaded rod as the positive electrode. The threaded rod was positioned parallel to the grounded plate and separated from the grounded plate by 5 cm. No corona discharges were observed (using de-ionized water). The current flowed to ground from multiple points along the rod. At no point along the rod was the field strength high enough to produce corona discharges. A contributing factor to the low field strength was the comparatively large diameter of the rod. Using a very fine wire in place of the rod might have yielded different results.

A third issue related to engineering development is design of an inexpensive, reliable, high voltage pulsed power supply. Design, construction, modification, and repair of the pulsed power supplies used in this investigation were the most costly and time-consuming parts of the effort.

A fourth issue is an economic one. If the major effect of pulsed corona discharges in aqueous solutions is the generation of hydrogen peroxide, then it is likely to be far more cost effective to buy hydrogen peroxide from a chemical supply company than to generate it using corona discharge technology.

ACKNOWLEDGEMENTS

The author wishes to thank Dr. Harold Guard, Environmental Applied Research Program Officer at the Office of Naval Research and Mr. Alex Lardis, Environmental Applied Research Program Manager at the Naval Surface Warfare Center, Carderock MD for their support. The author also wishes to express his appreciation to Mr. Ray Cappillino and Mr. Karlin Canfield for their assistance in building the experimental apparatus and Ms. Aviva Speceal for her assistance in conducting experiments.

REFERENCES

1. MEMORANDUM, From: J.W. Melone, Director, Chemical Management Division, EPA Headquarters, To: Regional Toxic Substances Division Director, Subj: *Disposal of Surfaces Covered With PCB Containing Coatings*, dated 21 Feb 1997.

2. "A Preliminary Study of Pulsed Streamer Corona Discharge for the Degradation of Phenol in Aqueous Solutions", by A.K. Sharma, B.R. Locke, et al, Hazardous Waste and Waste Materials, Vol. 10, No. 2, 1993.

3. "Nonequilibrium Volume Plasma Chemical Processing", by B. Eliasson and U. Kogelschatz, ABB Corporate Research, Baden Switzerland, IEEE Transactions on Plasma Science, Vol. 19, No. 6, Dec 1991.

4. "Computer Technique for Calculation of Potential Distribution in Multi-dielectric Media", by K.T. Huang, and B.R. Milner, TN-1502, Naval Civil Engineering Laboratory, 1977.

4. " Multi-dimensional Modeling of the Dynamic Morphology of Streamer Coronas", by P.A. Vitello, B.M. Penetrante, and J.N. Bardsley, High Temperature Physics Division, Lawrence Livermore National Laboratory, Non-Thermal Plasma Techniques for Pollution Control, Part A, NATO ASI Series, Springer-Verlag, Berlin 1993.

5. Physical Chemistry, by F. Daniels and R. Alberty, 2 nd edition, John Wiley & Sons, New York, 1962, P.73.

6. "Preliminary Investigation of Prebreakdown Phenomena and Chemical Reactions Using a Pulsed High-Voltage Discharge in Water", by J. Sidney Clements, Masayuki Sato, and Robert Davis, Florida State University, IEEE Transactions on Industrial Applications, Vol. IA-23, No. 2, April 1987.

7. "Critical Review of Rate Constants for Reactions of Hydrated Electrons, Hydrogen Atoms and Hydroxyl Radicals in Aqueous Solutions" by G.V. Buxton , C. L Greenstock, et al, Journal of Physical Chemistry Reference Data, Vol. 17, No. 2, 1988.

8. Personal communication between Prof. B.R. Locke, Florida State University, and R.E. Kirts, NFESC, Aug, 1998.

9. "The Effects of Carbon Particles on Aqueous Phase Pulsed Streamer Corona", by David R. Grymonpre', Masters Thesis, Florida State University, Tallahassee, FL., 1998.